

Targeted Nanoparticles for the Delivery of Novel Bioactive Molecules to Pancreatic Cancer Cells

Vanna Sanna, Salvatore Nurra, Nicolino Pala, Salvatore Marceddu, Divya Pathania, Nouri Neamati, and Mario Sechi

J. Med. Chem., **Just Accepted Manuscript** • DOI: 10.1021/acs.jmedchem.5b01571 • Publication Date (Web): 03 May 2016

Downloaded from <http://pubs.acs.org> on May 3, 2016

Just Accepted

“Just Accepted” manuscripts have been peer-reviewed and accepted for publication. They are posted online prior to technical editing, formatting for publication and author proofing. The American Chemical Society provides “Just Accepted” as a free service to the research community to expedite the dissemination of scientific material as soon as possible after acceptance. “Just Accepted” manuscripts appear in full in PDF format accompanied by an HTML abstract. “Just Accepted” manuscripts have been fully peer reviewed, but should not be considered the official version of record. They are accessible to all readers and citable by the Digital Object Identifier (DOI®). “Just Accepted” is an optional service offered to authors. Therefore, the “Just Accepted” Web site may not include all articles that will be published in the journal. After a manuscript is technically edited and formatted, it will be removed from the “Just Accepted” Web site and published as an ASAP article. Note that technical editing may introduce minor changes to the manuscript text and/or graphics which could affect content, and all legal disclaimers and ethical guidelines that apply to the journal pertain. ACS cannot be held responsible for errors or consequences arising from the use of information contained in these “Just Accepted” manuscripts.

Journal of Medicinal Chemistry

**Targeted Nanoparticles for the Delivery of Novel Bioactive Molecules
to Pancreatic Cancer Cells**

Vanna Sanna,^{†,||} Salvatore Nurra,[†] Nicolino Pala,[†] Salvatore Marceddu,[§] Divya Pathania,[⊥]

Nouri Neamati,^{‡,*} and Mario Sechi^{†,||,*}

[†]*Department of Chemistry and Pharmacy, University of Sassari, Italy, and* ^{||}*Laboratory of Nanomedicine, University of Sassari, c/c Porto Conte Ricerche, Alghero, Italy, and* [§]*Istituto di Scienze delle Produzioni Alimentari (ISPA), CNR, sez. di Sassari, Italy, and* [⊥]*Department of Pharmacology and Pharmaceutical Sciences, University of Southern California, School of Pharmacy, Los Angeles, CA, USA, and* [‡]*Department of Medicinal Chemistry, College of Pharmacy, Translational Oncology Program, University of Michigan, Ann Arbor, MI, USA*

KEYWORDS: Pancreatic Cancer; Ductal Adenocarcinoma; Anticancer Therapeutics; Quinazolinediones; Plectin-1; Polymeric Nanoparticles; Targeted Nanoparticles; Targeted Delivery

ABSTRACT

Pancreatic ductal adenocarcinoma (PDAC) is an aggressive disease with poor prognosis and limited therapeutic options. Therefore, there is an urgent need to identify new, safe and targeted therapeutics for effective treatment of late as well as early stage disease. Plectin-1 (Plec-1) was recently identified as specific biomarker for detecting PDAC at an early stage. We envisioned that multivalent attachment of nanocarriers incorporating certain drugs to Plec-1-derived peptide would increase specific binding affinity and impart high specificity for PDAC cells. Previously, we discovered a novel class of compounds (e.g. quinazolinones, QDs) that exert their cytotoxic effects by modulating ROS-mediated cell signaling. Herein, we prepared novel QD242-encapsulated polymeric nanoparticles (NPs) functionalized with a peptide (Cys-PTP) to selectively bind to Plec-1. Similarly, we prepared QD-based NPs densely decorated with an isatoic anhydride derivative (2ABA). Furthermore, we evaluated their impact on ligand binding and antiproliferative activity against PDAC cells. The targeted NPs resulted more potent than the nontargeted constructs in PDAC cells warranting further development.

INTRODUCTION

Pancreatic ductal adenocarcinoma (PDAC) is one of the most lethal forms of cancer worldwide.¹ It has been estimated that in 2015 about 53,000 people will be diagnosed with PDAC, and about 41,800 people will die of this disease in the United States,² with similar statistics in the European Union.³ The high mortality rate of PDAC patients is linked to an aggressive malignant character and extensive metastasis and late onset of clinical symptoms, leading to a late-stage detection and chemoresistance.^{1,4,5} In addition to radiotherapy and surgery, chemotherapy represents a significant therapeutic option, however with only modest benefits.^{1,5} First-line chemotherapy includes combination of folinic acid, 5-fluorouracil, irinotecan and oxaliplatin (FOLFIRINOX).⁶ The other option includes gemcitabine⁷ in combination with albumin-bound paclitaxel (nab-paclitaxel).⁸ Similar to nab-paclitaxel, other strategies consisting of targeting therapeutic payload to cancer cells through conjugation to a tumour-cell-specific ligands can be equally effective in treating PDAC.⁹⁻¹¹ Recently, we identified novel quinazolinone-based compounds (QDs)^{12,13} that target metabolic reprogramming and oxidative stress, the emerging hallmarks of cancer cells.¹⁴⁻¹⁸ These novel QD compounds alter the cellular bioenergetic characteristic of cancer cells resulting in cytotoxicity by Akt-directed generation of reactive oxygen species (ROS),¹² and inhibited the growth of tumors in a mouse xenograft model of PDAC.¹³ The lead compound effectively blocked the activation of three critical signaling pathways: Src, FAK, and STAT3.¹³ Due to limited therapeutic options for PDAC we designed a novel delivery system to increase bioavailability and efficacy of the lead compound, the 6-[(3-acetylphenyl)amino]quinazolinone-5,8-dione.^{12,13} Recently, we developed PEGylated ligand targeted polymeric biocompatible nanoparticles (NPs) recognizing the prostate cancer cells.¹⁹ Active targeting by NPs “decorated” with specific ligands such as antibodies, aptamers, peptides, and small molecules, is envisioned to provide the most effective therapy.^{9,20-28} Several ligand-targeted nanotherapeutics are either approved or under clinical evaluation.^{11,25,28} Membrane receptors with significantly higher expression on cancer versus normal cells are suitable targets for therapeutic intervention.²⁹

1
2
3 Functionalization of NPs with ligands targeting the extracellular domain of these receptors can
4
5 enable selective delivery of therapeutic payload to tumor cells.²³⁻²⁸
6

7 For example, Plectin-1 (Plec-1), a high molecular weight protein (~500 kDa) that links intermediate
8
9 filaments to microtubules and microfilaments, has an important function in tumor pathogenesis.³⁰ It
10
11 has been shown that Plec-1 levels are low in normal pancreatic ductal cells, but its expression is
12
13 upregulated in PDAC.³¹ Importantly, Plec-1 exhibits distinct cytoplasmic and nuclear localization in
14
15 normal fibroblasts, whereas an aberrant expression on the cell membrane with cell surface
16
17 localization is observed in PDAC. Moreover, Plec-1 was suggested as a useful biomarker for
18
19 PDAC.³¹
20
21

22 Previously, Weissleder *et al.* developed proof-of-concept targeted magnetofluorescent NPs
23
24 composed of Plec-1 targeted peptides (PTP) for imaging of PDAC.³² The same group reported on
25
26 the development of magnetofluorescent reporters as a novel nanomaterial for biomedical
27
28 application.³³ Moreover, a nonspecific targeting ligand, the isatoic anhydride with its corresponding
29
30 isatoic nanoconjugate (i.e., 2-aminobenzoic-carboxylic-coated magnetic NPs), showed higher
31
32 uptake in cancer versus normal cells.³³
33
34

35 Here, we report on design and preparation of novel biocompatible NPs encapsulating QD242 (**1**),¹²
36
37 covered by small organic molecules (2ABA, **11**) or peptides (Cys-PTP, **12**) as targeting ligands
38
39 (Figure 1) in their polymeric shell surface to selectively bind to Plec-1 or to nonspecifically target
40
41 PDAC cells. We used *pseudo*-di-block-copolymer PLGA-**11** as well as the parent PLGA-A, and
42
43 *pseudo*-tri-block-copolymer PLGA-PEG-**12** and the parent PLGA-PEG-NH₂ to generate two sets of
44
45 200-300 nm size targeted and nontargeted (**1**)-encapsulated NPs (Figure 1). These NPs were
46
47 characterized for drug-content, drug-release, binding affinity, and cytotoxicity in MIA PaCa-2 cells.
48
49
50
51
52
53
54
55
56
57
58
59
60

RESULTS AND DISCUSSION

Design of targeted NPs

We incorporated a representative ROS-inducing compound, 6-{{4-(phenylcarbonyl)phenyl}amino}quinazoline-5,8-dione (**1**, Figure 1),¹² into a polymeric NPs conjugated to 2-amino-*N*-(3-aminopropyl)benzamide (**11**) as well as a targeting peptide (**12**, amino acid sequence: KTLLPTPC, Figure 1).^{32,33} Compound **1** produced IC₅₀ value of 1.6 ± 0.2 μM in MIA PaCa-2 cells¹² and is well suited as a model drug for nanoformulation. It carries a lipophilic benzoyl substituent instead of an acetyl group on the lead compound (i.e., 6-[(3-acetylphenyl)amino]quinazoline-5,8-dione) on the aminophenyl side chain. We chose poly(D,L-lactide-co-glycolide) carboxylic acid (PLGA-COOH, namely PLGA-A) and a poly(ethylene glycol) derivative, PLGA-PEG-NH₂, as polymer systems because of their well-established safety profile.^{34,35}

Initially, we used the 2-aminobenzoic-carboxylate conjugated with the aminopropane linker (**11**, Figure 1) as nonspecific PDAC targeting ligand, to obtain an intermediate to react with activated PLGA-NHS. The 2-aminobenzoic-carboxylic was derived from isatoic anhydride (Scheme 2).

The PTP peptide (amino acid sequence: KTLLPTP), identified using peptide phage display, targets Plec-1 with a high affinity and specificity.³² We decided to use the cysteine-containing PTP (**12**, Figure 1) because it can react with maleimide terminal groups of PEG in the PLGA-PEG-maleimide (i.e., PLGA-PEG-mal). PEGylation confers immune shielding and “stealth” properties to NPs and is a suitable spacer to maintain an optimal distance between the targeting ligand and the NP surface.

We also efficiently synthesized the targeting ligand **11** as well as PLGA-**11**, PLGA-PEG-NH₂, PLGA-PEG-mal, and PLGA-PEG-**12** that are required for the NP formulation. To obtain a better control of **11** and **12** functionalization, we conjugated these ligands to their respective polymeric systems (i.e., PLGA-**11** and PLGA-PEG-**12**) prior to nanoformulation.

Synthesis of **1**

Compound **1** (Scheme 1) was synthesized using Bracher's methodology with slight modifications to our previously reported procedure.¹² Regioselective substitution of quinazoline-5,8-dione (**2**) with 4-aminobenzophenone (**3**) in the presence of Ce(III) ions gave **1** as expected. The key synthon **2** was synthesized starting from the readily available 2,5-dimethoxybenzaldehyde (**4**), which was nitrated with concentrated nitric acid in the presence of acetic anhydride under magnetic stirring affording the 3,6-dimethoxy-2-nitrobenzaldehyde (**5**). The acid-catalyzed cyclization of this regioisomer by exposing it to gaseous HCl led to the formation of the diformamido-derivative **6**, which was then cyclized to 5,8-dimethoxyquinazoline (**7**) by treatment with zinc powder and acetic acid. Final oxidation by cerium ammonium nitrate gave the compound **2** (Scheme 1B). It is worth noting that, the nitration reaction, using nitric acid/acetic anhydride in mild condition, gives higher yield than a previously reported condition¹² using a molar excess of silica gel supported nitric acid (68% vs 50-58%, respectively). Moreover, similar results were observed by the oxidation of **7** to **2** with cerium ammonium nitrate in acetonitrile/water solution. These modifications led to a 2-fold improvement in overall yield of the key synthon **2**. Compound **1** and the intermediates were fully characterized by NMR, MS, and elemental analyses.

Synthesis of **11**

The intermediate *tert*-butyl (3-(2-aminobenzamido)propyl)carbamate (**10**) was prepared by treating isatoic anhydride (**9**) with *tert*-butyl (3-aminopropyl)carbamate (**8**) in the presence of potassium carbonate and THF at 70 °C with 74% yield (Scheme 2). The *tert*-butyloxycarbonyl (Boc) group of **10** was removed with 50% trifluoroacetic acid (TFA) in CH₂Cl₂ solution at room temperature to obtain the desired ligand **11**, which was characterized by NMR, MS, and elemental analyses.

Synthesis of *pseudo*-di-block-copolymer PLGA-11

Block-copolymers are effectively used as pre-conjugated starting materials for the preparation of

1
2
3 precisely engineered NPs targeted nanoconjugates for cancer therapy.^{24,36-38} Conjugation of the
4
5 terminal amine group of **11** ligand with the activated electrophilic NHS esters of PLGA carboxylic
6
7 acids (e.g., PLGA-A) allows the formation of physiologically stable amide bonds. The designed
8
9 PLGA-**11** copolymer and di-block-copolymers were synthesized in a two-step reaction.
10
11 Specifically, the amine functional groups of **11** were reacted with the carboxy-capped PLGA-NHS
12
13 in DMF in the presence of DIPEA (Scheme 3, stage 1). The activated amine-reactive NHS-ester of
14
15 PLGA (PLGA-NHS) was prepared by treating PLGA-A with EDC/NHS in an organic solvent at
16
17 room temperature (Scheme 3). As expected, the ¹H-NMR analysis revealed aromatic peaks in the
18
19 range 6.5-8.0 ppm, corresponding to proton pattern of **11** (S25). The successful conjugation of **11** to
20
21 PLGA polymer also was supported by two absorption bands in 190 and 255 nm regions as depicted
22
23 in the UV chromatogram (Figure 2).
24
25
26
27
28

29 **Synthesis of di-block-copolymer of PLGA-PEG-NH₂ and PLGA-PEG-mal**

30
31 NPs should ideally have a favourable hydrophobic/hydrophilic balance on their surface in order to
32
33 a) have a minimal self-self and self-nonsel self interaction, b) escape capture by the reticuloendothelial
34
35 system (RES) to ensure immune evasion, c) reduce opsonization, d) facilitate efficient clearance of
36
37 materials from the body, and d) prevent nanoparticle loss to undesired location. PEGylation
38
39 constitutes a suitable strategy for this purpose, and the preparation of PEGylated NPs is well
40
41 documented.³⁹⁻⁴¹ PLGA-PEGs are usually synthesized by conjugation or polymerization of PEG to
42
43 PLGA *via* standard carbodiimide/NHS-mediated chemistry.^{37,41,42}
44
45
46

47 The starting polymer PLGA-PEG-NH₂ and the carboxylate-functionalized di-block-copolymer
48
49 PLGA-PEG-mal (Scheme 4 and Scheme 5, stage 1, respectively) were prepared by conjugating
50
51 bifunctional PEGs, NH₂-PEG-NH₂ or NH₂-PEG-mal, to activated PLGA-A. The structure of
52
53 copolymers was confirmed by ¹H-NMR spectroscopy. Specifically, signals centered at 1.58 ppm for
54
55 both polymers are attributed to the lactide methyl repeat units (resonance shift **a**, Schemes 4 and 5).
56
57 Overlapping multiplets observed in the range 5.10-5.32 and 4.63-4.96 indicate the lactide methine
58
59
60

1
2
3 (b, Schemes 4 and 5) and the glycolide protons (c, Schemes 4 and 5), respectively. In addition to the
4 defined signals for PLGA, the presence of the peak at 3.64/3.65 ppm (for NH₂-PEG-mal and NH₂-
5 PEG-NH₂, respectively), corresponding to the PEG methylene protons (d, Schemes 4 and 5),
6 confirmed the successful preparation of both polymers.
7
8
9
10

11 12 13 14 **Synthesis of *pseudo*-tri-block-copolymer PLGA-PEG-12**

15
16 We obtained a prefunctionalized biopolymer, PLGA-PEG-12, to avoid the postparticle
17 modifications. The peptide 12 was prepared by fluorenylmethyloxycarbonyl- (Fmoc)-based solid-
18 phase peptide synthesis (Supporting Information, S29-S32). Conjugation of the targeting agent, i.e.
19 12, to carboxylate PEG terminal group was performed using the electrophilic maleimide
20 functionality of PEG activated carboxylic acids. Reaction between the terminal SH group of 12 with
21 PEG-mal resulted in the formation of physiologically stable S-C bonds. The designed *pseudo*-tri-
22 block-copolymer, PLGA-PEG-12 copolymer, was synthesized using a two-step reaction (Scheme 5,
23 stage 1) as described above for the preparation of the di-block-copolymer. The ¹H-NMR spectrum
24 recorded for PLGA-PEG-12 revealed resonance shifts at 1.58, 3.64, 4.64-4.88, and 5.10-5.28 ppm
25 characteristics of PLGA-PEG backbone. Moreover, it also shared a series of partially overlapped
26 multiple peaks (Figure S27), especially in the aliphatic zone, attributable to the 12 signal pattern
27 (Figure S32). Furthermore, the strong absorption bands in 245 nm region observed in the UV
28 chromatogram (Figure 3), support the successful conjugation of 12 to PLGA-PEG copolymer.
29 Further characterization analyses such as molecular weights, refractive and polydispersity indexes,
30 were assessed by gel permeation chromatography (GPC) - size exclusion chromatography (SEC)
31 (see in Supporting Information for details).
32
33
34
35
36
37
38
39
40
41
42
43
44
45
46
47
48
49
50
51

52 53 54 **Nanoformulation and Characterization of Nontargeted and Targeted NPs**

55
56 In the present study, we used PLGA-A, PLGA-PEG-NH₂, PLGA-11, and PLGA-PEG-12 polymer
57 systems to fabricate nontargeted and targeted NPs as novel constructs and suitable carriers for
58
59
60

1
2
3 PDAC therapy. The PLGA was chosen owing to its physicochemical properties as well as its
4 biocompatibility and biodegradability. Moreover, modification of the NP' surface with PEG enables
5 nonspecific interactions reduction, prolonging circulation time, and increasing accumulation in
6 tumors due to the enhanced permeability and retention (EPR) effect.⁴³⁻⁴⁶ In particular, the
7 hydrophilic ethylene glycol repeats of PEG confer to NPs enhanced solubility in serum, with
8 reduced RES uptake and prolonged circulation time with respect to uncoated counterparts.^{47,48}
9
10 Moreover, grafting with PEG prevents NP aggregation by increasing hydrophilicity via ether
11 repeats, which form hydrogen bonds with solvent, and by modulating the steric distance and the
12 amount of attraction between NPs, as well as those between tissue proteins and NPs. Modulation of
13 the NP flexibility and the reduced accumulation in the liver are other key factors that influence
14 extravasation, thus allowing for a favourable modulation of EPR effect.⁴⁸
15

16
17 To optimize the fabrication of NPs and to ensure rapid precipitation of batches containing the
18 hydrophilic PLGA-PEG co-polymer, we used poly(epsilon-caprolactone) (PCL) mixture with
19 PEGylated polymers to prepare PLGA-PEG-NH₂ and PLGA-PEG-12 NPs. PCL is useful for
20 controlled and sustained drug delivery due to its tunable mechanical properties, high permeability
21 and low toxicity.⁴⁹⁻⁵¹
22

23
24 All batches of (1)-encapsulated NPs were successfully prepared using a modified nanoprecipitation
25 method as described (Figure 1, Schemes 3 and 5, stage 2).^{19,51} During the precipitation in water, the
26 polymers self-assembles to form NPs, in which the hydrophobic PLGA blocks would interact with
27 the PCL into a core, thus minimizing their exposure to aqueous surroundings. Simultaneously, the
28 hydrophilic COOH/NH₂ surface or PEG-NH₂ and PEG-12 flexible moieties extend from the shell to
29 stabilize the core by preventing degradation and aggregation.
30

31
32 NPs generated from both polymer systems (i.e. PLGA- and PLGA-PEG-based NPs) were
33 characterized for surface morphology with SEM, particle size, zeta potential and encapsulation
34 efficiency (Table 1).
35

36
37 Figure 4 shows representative SEM images of PLGA-A- (a), PLGA-11- (b), PLGA-PEG-NH₂/PCL-

1
2
3 (c), and PLGA-PEG-**12**/PCL- (d) (**1**)-loaded NPs. All particles were characterized by similar
4 morphological properties having smooth surface and spherical shape, and unimodal distribution.
5 However, the NPs have different mean diameters [PLGA- (155.8 and 220.1 nm, for PLGA-A- and
6 PLGA-**11** NPs, respectively) and PLGA-PEG/PCL- (353.5 and 328.0 nm, for PLGA-PEG-
7 NH₂/PCL- PLGA-PEG-**12**/PCL NPs, respectively)] (Table 1 and Figure 4a-d).
8
9

10
11
12
13
14 The zeta potential was negative for PLGA-A NPs due to the negatively charged carboxyl groups on
15 the terminal of PLGA-A. PLGA-PEG-NH₂-, PLGA-**11**- and PLGA-PEG-**12** NPs showed zeta
16 potential between 10 and 14 mV due to their surface amine or amino acid functionalities (Table 1).
17
18

19
20 Our statistical analysis highlighted that the amount of **1** loaded was significantly higher ($p < 0.05$)
21 for PLGA-PEG-NH₂- and PLGA-PEG-**12** NPs (ranging from 20% to 24%) than that for PLGA-A-
22 and PLGA-**11** NPs (Table 1). This difference is perhaps due to the higher hydrophilicity of the PEG
23 conjugated polymer than that of PLGA counterparts.
24
25

26
27 We obtained 50 to 69% yield for all preparations over multiple experiments. The PLGA-PEG/PCL
28 polymeric blended NPs produced encapsulation efficiency values ranging from 64% (for PLGA-
29 PEG-NH₂/PCL NPs) to 69% (for PLGA-PEG-**12**/PCL NPs). The PLGA-based nanosystems yields
30 were 50 and 55%, for PLGA-A- and PLGA-**11** NPs, respectively. These differences can be
31 attributed to the presence of the hydrophobic PCL and PLGA chains and the hydrophilic PEG
32 moieties that can facilitate the incorporation of bioactive molecules into the polymeric matrix.
33
34 Additionally, to evaluate the cellular uptake of the NPs, four batches (PLGA-A-, PLGA-PEG-NH₂-,
35 PLGA-**11**- and PLGA-PEG-**12** of fluorescent 6-coumarin (6C)-encapsulated NPs were obtained and
36 characterized using the above-mentioned method (Table S34).
37
38
39
40
41
42
43
44
45
46
47
48
49
50
51

52 ***In Vitro* Kinetic Release of **1** from NPs**

53
54 The *in vitro* release profiles of compound **1** from NPs is depicted in Figure 5. The experiments were
55 performed in phosphate-buffered saline (PBS) at pH 6.5 and 7.4 to simulate both the slightly acidic
56 microenvironment of extracellular fluid in most tumors and the physiological conditions in normal
57
58
59
60

1
2
3 tissues, respectively.¹⁹ The experiments were carried out by direct determination of **1** from different
4
5 types of NPs in the release medium. The cumulative amount of **1** released from NPs indicated that
6
7 the nanoencapsulation resulted in an effective release rate of **1** under both experimental conditions
8
9 (i.e., PBS, pH 6.5 and 7.4, Figure 5a, and 5b, respectively). Nanoparticle formulations showed a
10
11 similar release behaviour, and this suggests that the pH of the medium did not significantly affect
12
13 the release of **1** from the nanoformulations. In particular, PLGA-A-, PLGA-**11** NPs, and PLGA-
14
15 PEG-NH₂ NPs in both media shared similar kinetic release profiles. We observed a near 90%
16
17 release of **1** from PLGA-PEG-NH₂ NPs within the first 2 h and a complete release within 4-6 h. We
18
19 observed only 45-50% release of **1** from PLGA-PEG-**12** NPs within 3 h in both acidic and
20
21 physiological medium, and about 70-80% at 6 h. A possible explanation for this difference could be
22
23 due to the presence of peptide **12** in PEGylated NPs potentially affecting degradation kinetics. More
24
25 specifically, during the generation of NPs, the PLGA block can interact with PCL to produce a
26
27 hydrophobic core. This construct might play a major role in stabilizing the core, whereas the other
28
29 part of PEG-**12** protrude from the particle surface, forming an external hydrophilic *pseudo*-shield,
30
31 and thus preventing degradation.
32
33
34
35
36
37

38 **Inhibition of cell proliferation**

39
40 We compared the cytotoxicity of the targeted (**1**)-encapsulated NPs (PLGA-**11** and PLGA-PEG-**12**
41
42 NPs) with those of the nontargeted particles (PLGA-A and PLGA-PEG-NH₂) in MIA PaCa-2 cells
43
44 using MTT assay (Figure 6). The PLGA-**11** and PLGA-PEG-**12** (**1**)-loaded NPs showed 70% and
45
46 87% growth inhibition, respectively. The nontargeted PLGA-A and PLGA-PEG-NH₂ NPs showed
47
48 <30% and <50% growth inhibition (Figure 6), suggesting that targeted NPs are significantly more
49
50 effective than the nontargeted particles. In particular, we observed an improved antiproliferative
51
52 activity for targeting Plec-1 by peptide **12** with (**1**)-loaded NPs. This behaviour can be attributed to
53
54 an active targeting to Plec-1 promoting an enhanced binding between NPs and the cells, thus
55
56 resulting in increased accumulation and cell uptake through receptor mediated endocytosis.
57
58
59
60

Surface plasmon resonance (SPR) binding assays

The ability of the most effective anti-Plec-1 targeted NPs (PLGA-PEG-**12** NPs) to specifically bind Plec-1 protein, in comparison with the nontargeted ones (PLGA-PEG-NH₂ NPs), was assessed by real-time interaction analysis using surface plasmon resonance (SPR) experiments.⁵² Kinetic and affinity evaluation and determination of binding specificity were conducted by immobilizing the Plec-1 protein on a sensor surface. The analyte (PLGA-PEG-**12** NPs or PLGA-PEG-NH₂ NPs) was injected in solution over the surface. Changes in SPR response were analyzed, providing affinity binding results, expressed as response units (RU). A difference of about 350-400 RU was observed for NPs with and without peptide **12** (Figure 7), with a significant increase in response units (RU) for PLGA-PEG-**12** NPs compared to PLGA-PEG-NH₂ NPs for binding to Plec-1. Indeed, sensorgrams revealed a slow association and dissociation processes. These results demonstrate good affinity for **12** targeted NPs toward Plec-1 protein, with only a residual interaction provided by the nontargeted NPs, thus supporting that this specific interaction can significantly contribute to the growth inhibition of MIA PaCa-2 cells by (**1**)-loaded NPs.

Cellular Uptake

The correlation between antiproliferative activity of the (**1**)-loaded NPs with cellular uptake by the cancer cells was further corroborated by internalization of 6-coumarin-loaded NPs, which were visualized by fluorescence microscopy. Figure 8 shows images (20x magnification) of cellular uptake efficiency of nontargeted and targeted NPs. In particular, after 1 h incubation, the targeted PLGA-**11** and PLGA-PEG-**12** NPs showed higher cellular uptake than PLGA-A and PLGA-PEG-NH₂, respectively, with strong fluorescence in perinuclear space, thus confirming their accumulation and sustained retention by the cells.

CONCLUSIONS

Previously, we discovered a novel class of compounds displaying ROS-mediated decrease in Src/FAK and STAT3 phosphorylation resulting in efficient inhibition of cell proliferation, adhesion, and migration, ultimately leading to apoptosis. In an attempt to improve their pharmacological, PK, and distribution properties we used a novel nanotechnology platform to selectively deliver our novel ROS-inducing compounds to PDAC cells.

We demonstrated that the MIA PaCa-2 cells are more sensitive to the targeted than the nontargeted particles. Furthermore, we observed that the targeted (**1**)-loaded NPs (PLGA-**11** and PLGA-PEG-**12**) efficiently bind to MIA PaCa-2 cells. In particular, these data indicate that functionalization of the NPs surface with peptides to selectively bind to Plec-1 or with nonspecific small molecules as targeting ligands, efficiently increase their adhesion and uptake in PDAC cells in comparison to the nonfunctionalized particles. As expected, the NPs targeting Plec-1 demonstrated to be the most effective prototypes. These results also support the hypothesis that the primary role of targeting agents is to increase cellular uptake of NPs and their loading into tumor cells. These insights might constitute a suitable translational platform for development of powerful therapeutic tools to treat pancreatic cancer.

EXPERIMENTAL SECTION

Materials

Poly(D,L-lactide-co-glycolide) carboxylic acid end group, (PLGA-A, Purasorb Polymer PDLG 5002A, Mw ~17,000) (lactide/glycolide ratio of 50:50, viscosity range: 0.20 dL/g in CHCl₃) was kindly provided by Corbion Purac (Gorinchem, The Netherlands). Poly(epsilon-caprolactone) (PCL, Mw ~80,000), polyvinyl alcohol (PVA, Mw Mw 31,000–50,000), and 6-coumarin were purchased from Sigma-Aldrich (Steinheim, Germany). The heterobifunctional PEG polymer with a terminal amine and carboxylic acid functional group, NH₂-PEG-COOH (Mw = 3400), the homobifunctional PEG polymers with both terminal amines NH₂-PEG-NH₂ (HCl salt, Mw = 3500), and with a terminal amine and maleimide functionality NH₂-PEG-mal (TFA salt, Mw = 3500), were purchased from JenKem Technology USA. The anti Plec-1 peptide (KTLLPTPC, **12**, lyophilized trifluoroacetate salt) was purchased from CASLO Laboratory ApS, c/o Scion Denmark Technical University, Lyngby, Denmark. The peptide was prepared by (Fmoc)-based solid-phase peptide synthesis using H-Cys(Trt)-CTC Resin (Supporting Information, S29). The peptide **12** was purified by preparative reversed-phase high performance liquid chromatography (RP-HPLC) and quality controlled by analytical HPLC and mass spectrometry (see in Supporting Information for details, S29-S32).

All solvents and other chemicals (used for the preparation of **1**) were purchased from Sigma-Aldrich or Carlo Erba (analytical grade and were used without further purification). Melting points (mp) were determined using an Electrothermal melting point or a Köfler apparatus and are uncorrected. Nuclear magnetic resonance (¹H-NMR, ¹³C-NMR) spectra were determined in CDCl₃, DMSO-*d*₆ or CDCl₃/DMSO-*d*₆ (in 3/1 ratio) and were recorded on 400 MHz Bruker Avance III. Chemical shifts are reported in parts per million (ppm) downfield from tetramethylsilane (TMS), used as an internal standard. Splitting patterns are designated as follows: s, singlet; d, doublet; t, triplet; q, quadruplet; m, multiplet; brs, broad singlet; dd, double doublet. The assignment of

exchangeable protons (*OH* and *NH*) was confirmed by the addition of D₂O. Mass spectra were obtained on a triple-quadrupole QqQ Varian 310-MS mass spectrometer, a Hewlett-Packard 5989 Mass Engine Spectrometer, or a MALDI micro MX (Waters, Micromass) equipped with a reflectron analyser. Analytical thin-layer chromatography (TLC) was carried out on Merck silica gel F-254 plates. Flash chromatography purifications were performed on Merck Silica gel 60 (230-400 mesh ASTM) as a stationary phase. Molecular weights, polydispersity and refractive indexes of polymers were determined by GPC-SEC using the instrument Viscotek 270 (for SEC-TDA, Alfatest, Italy), and were performed by Alfatestlab s.r.l. (Cinisello Balsamo, Mi, Italy). The purity of copolymers was determined by HPLC using an HP 1200 (Agilent Technologies, USA) system, equipped with a Hypersil BDS C18 column (Alltech Italy, 250 × 4.6 mm i.d., 5 μm particle size); these materials were found to be >95% pure. Elemental analyses for **1**, **11**, and for all intermediates, were performed on a Perkin-Elmer 2400 spectrometer at Laboratorio di Microanalisi, Dipartimento di Chimica, Università di Sassari (Italy), and were within ±0.4% of the theoretical values.

Synthesis of 6-**{4-(phenylcarbonyl)phenyl}amino**quinazoline-5,8-dione (**1**)

A solution of quinazoline-5,8-dione (**2**, 0.22 g, 1.37 mmol), cerium (III) chloride heptahydrate (CeCl₃·7H₂O, 1.1 eq), and 4-aminobenzophenone (**3**, 1.1 eq.) in absolute ethanol (20 mL) was stirred at room temperature for 3 h. Next, most of the ethanol was removed under vacuum, and water was added, followed by extraction with CH₂Cl₂. The organic layer was washed with water and brine, dried over anhydrous sodium sulfate, and concentrated to dryness. The crude product was purified by flash chromatography (eluent: ethyl acetate) to give the expected product. Red-brown solid. Yield: 79%; mp 233-234 °C (lit. mp 233-236 °C).¹² ¹H-NMR (400 MHz, CDCl₃): δ 9.70 (s, 1H, H₄), 9.54 (s, 1H, H₂), 7.93 (d, 2H, Ar-H), 7.80 (d, 2H, Ar-H), 7.75 (s, 1H, NH), 7.64–7.61 (m, 1H, Ar-H), 7.54–7.51 (m, 2H, Ar-H), 7.41 (d, 2H, Ar-H), 6.85 (s, 1H, H₈). ¹³C-NMR (100 MHz, CDCl₃): δ 195.04, 180.77, 180.42, 163.87, 156.59, 153.99, 143.44, 140.25, 137.27, 132.71, 132.08, 129.93, 128.48, 123.29, 121.69, 106.37. MALDI-TOF: m/z 354 [M]⁺.

Quinazoline-5,8-dione (2)

A solution of 5,8-dimethoxyquinazoline (**7**, 0.50 g, 2.63 mmol) in (7:3) acetonitrile:water (13 mL) was cooled at 0 °C in an ice bath and a solution of ceric ammonium nitrate [(NH₄)₂Ce(NO₃)₆ (2.7 eq) (9:1) acetonitrile:water (13 mL) was added dropwise. The reaction mixture was stirred for 20 min and, after monitoring with TLC (CHCl₃/CH₃OH 9.5:0.5), poured into ice/water and extracted with CH₂Cl₂. Then, the organic layer was washed with water, dried over anhydrous sodium sulfate, and concentrated to dryness to give **2** as brown powder. Yield: 69%. mp: > 320 °C. (lit. mp: > 320 °C). ¹H-NMR (400 MHz, DMSO-d₆): δ 9.68 (s, 1H), 9.43 (s, 1H), 7.28 (d, 1H), 7.18 (d, 1H). ¹³C-NMR (100 MHz, DMSO-d₆): δ 184.07, 182.88, 162.08, 156.27, 152.60, 139.46, 137.74, 124.61. ESI: *m/z* 161 [M+1]⁺.

5,8-dimethoxyquinazoline (7)

Zinc powder (8.18 g, 125.13 mmol, 15.15 eq) was added to a suspension of N,N'-[(3,6-dimethoxy-2-nitrophenyl)methylene]difformamide (**6**, 2.5 g, 8.26 mmol) in triturated ice (30 g) and glacial acetic acid (11.5 mL), under constant magnetic stirring. The reaction mixture was stirred for 2 h in ice bath, and for 4 h at room temperature. Next, the reaction mixture was dropped (through filter paper) on cooled 50% NaOH (45 mL), and the yellow colored suspension thus formed was left without stirring for 1 h. Then, the suspension was filtered to give a yellow powder, which was solubilized in ethyl acetate, filtered, dried over anhydrous sodium sulfate, and concentrated to dryness yielding the desired compound **7**. Yield: 91%. mp: 116-117 °C. (lit. mp 116-119 °C). ¹H-NMR (400 MHz, DMSO-d₆): δ 9.64 (s, 1H), 9.28 (s, 1H), 7.38 (d, 1H), 7.09 (d, 1H), 3.98 (s, 3H), 3.94 (s, 3H). ¹³C-NMR (100 MHz, DMSO-d₆): δ 154.88, 154.49, 148.35, 148.02, 141.60, 117.16, 113.59, 106.14, 56.11. GC-MS: *m/z* 190 [M]⁺.

N,N'-[(3,6-dimethoxy-2-nitrophenyl)methylene]diformamide (6)

A solution of 3,6-dimethoxy-2-nitrobenzaldehyde (**5**, 4.0 g, 18.94 mmol) in formamide (H₂NCHO, 66.5 eq.), heated at 40 °C, was exposed to dry HCl gas (1 h) until the temperature reached 80 °C. Then, the solution was cooled to room temperature, and water/ice was added. Pale yellow precipitate was formed, which was filtered, dried and triturated with ethyl acetate and petroleum ether to yield the desired compound **6**. Yield: 90%. mp: 254-255 °C (lit. mp 254 °C).¹² ¹H-NMR (400 MHz, DMSO-d₆): δ 8.67 (d, 2H), 7.92 (s, 2H), 7.28 (s, 2H), 6.77 (t, 1H), 3.88 (s, 3H), 3.82 (s, 3H). NMR (100 MHz, DMSO-d₆): δ 160.17, 150.77, 143.64, 139.60, 119.59, 114.33, 113.94, 57.02, 56.64, 48.51. ESI: *m/z* 284 [M+1]⁺.

3,6-Dimethoxy-2-nitrobenzaldehyde (5)

Nitric acid (91.83 mmol, 7.63 eq), acetic anhydride (43.31 mmol, 3.6 eq) and 2,5-dimethoxybenzaldehyde (**4**, 1.3 g, 12.03 mmol) were added at 0 °C with stirring, respectively. After 1.5 h stirring, the mixture was poured onto 10 mL ice/water. The resulting yellow solid was filtered, washed with cold water and then purified by flash chromatography on silica gel using ethyl acetate-petroleum ether (1:1) to give first the regioisomer 2,5-dimethoxy-4-nitrobenzaldehyde, and then (by further elution with only ethyl acetate), the desired compound **5**. Yield: 68%. mp 165-167 °C (lit. mp 163-165 °C and 159 °C).¹² ¹H-NMR (400 MHz, DMSO-d₆): δ 10.26 (s, 1H), 7.70 (d, 1H), 7.49 (d, 1H), 3.96 (s, 3H), 3.87 (s, 3H). ¹H-NMR (400 MHz, CDCl₃): δ 10.39 (s, 1H), 7.30 (d, 1H), 7.12 (d, 1H), 3.97 (s, 3H), 3.89 (s, 3H). ¹³C-NMR (100 MHz, DMSO-d₆): δ 186.69, 166.22, 154.21, 153.42, 148.42, 123.73, 116.48, 57.14, 57.02. GC-MS: *m/z* 211 [M]⁺.

Synthesis of 2-amino-N-(3-aminopropyl)benzamide (11)

The intermediate *tert*-butyl (3-(2-aminobenzamido)propyl)carbamate (**10**, 0.23 g, 0.78 mmol) was dissolved in 20 mL of 1:1 TFA and CH₂Cl₂ solution in an ice bath (0 °C), and stirred at room temperature for 3 h. Then, the resulting solution was evaporated under reduced pressure. The

1
2
3 colorless residue was triturated with dry diethyl ether to yield the desired compound **11** as brown oil
4 (yield, 100%). ¹H-NMR (400 MHz, DMSO-d₆): δ 8.38 (brs, 1H, CO-NH), 7.79 (brs, 3H, NH₃⁺),
5 7.50 (d, 1H, Ar-H), 7.18 (t, 1H, Ar-H), 6.75 (d, 1H, Ar-H), 6.59 (t, 1H, Ar-H), 3.29 (d, 2H, NH-
6 CH₂), 2.84 (d, 2H, CH₂-NH₂), 1.79 (t, 2H, CH₂). ¹³C-NMR (100 MHz, DMSO-d₆): δ 169.02,
7 148.25, 131.75, 128.04, 116.96, 115.51, 115.38, 36.91, 35.83, 27.42 (CF₃COOH, 158.84, 158.49,
8 158.13, 157.78, 120.26, 117.37, 114.46, 111.55). MALDI-TOF: *m/z* 193 [M⁺].
9
10
11
12
13
14
15
16
17

18 19 **Synthesis of *tert*-butyl (3-(2-aminobenzamido)propyl)carbamate (10)**

20 A mixture of isatoic anhydride (**9**, 0.22 g, 1.38 mmol), *tert*-butyl (3-aminopropyl)carbamate (**8**, 0.2
21 mL, 1.15 mmol), and potassium carbonate (0.32 g, 2.30 mmol, 2.0 eq) in anhydrous THF (3 mL)
22 was stirred at 70 °C for 20 h under nitrogen atmosphere. After cooling, water was added and stirring
23 was continued for 4 h. The reaction mixture was concentrated and extracted with ethyl acetate,
24 dried over Na₂SO₄, then concentrated and triturated to give a white powder (yield, 74%). mp 80-81
25 °C. ¹H-NMR (400 MHz, DMSO-d₆): δ 8.15 (brs, 1H, CO-NH), 7.44 (d, 1H, Ar-H), 7.12 (t, 1H, Ar-
26 H), 6.80 (brs, 1H, NH-CO), 6.68 (d, 1H, Ar-H), 6.52 (t, 1H, Ar-H), 6.36 (s, 2H, Ar-NH₂), 3.20-3.19
27 (m, 2H, NH-CH₂), 2.97-2.96 (m, 2H, CH₂-NH₂), 1.62-1.58 (m, 2H, CH₂), 1.38 (s, 9H, CH₃). ¹³C-
28 NMR (100 MHz, DMSO-d₆): δ 168.78, 155.57, 149.50, 131.49, 127.90, 116.26, 114.86, 114.49,
29 77.45, 37.69, 36.44, 29.58, 28.23. MALDI-TOF: *m/z* 293 [M⁺].
30
31
32
33
34
35
36
37
38
39
40
41
42
43
44

45 **Synthesis of PLGA-NHS**

46 PLGA-NHS was prepared (yield, 94%) by using the previously reported procedure,¹⁹ and with the
47 following conditions: PLGA-A (3.0 g, 0.166 mmol), *N*-hydroxysuccinimide (NHS, 0.077 g, 0.714
48 mmol) and 1-ethyl-3-(3-dimethylaminopropyl)carbodiimide (EDC, 0.14 g, 0.664 mmol). ¹H-NMR
49 (400 MHz, CDCl₃): δ 5.23-5.20 (m, 1H, -OC-CH(CH₃)O-, PLGA), 4.90-4.70 (m, 2H, -OC-CH₂O-,
50 PLGA), 1.58 (brs, 3H, -OC-CH(CH₃)O-, PLGA).¹⁹
51
52
53
54
55
56
57
58
59
60

Synthesis of *pseudo*-di-block-copolymer PLGA-11

To a solution of PLGA-NHS (0.50 g, 0.028 mmol) in anhydrous dimethylformamide (DMF, 3 mL), a solution of **11** (0.034 g, 0.111 mmol) in DMF (1.5 mL) and *N,N*-diisopropylethylamine (DIPEA, 0.90 mL, 5.16 mmol) were added. The resulting mixture was magnetically stirred at room temperature for 24 h under nitrogen atmosphere. The desired *pseudo*-di-block-copolymer PLGA-11 was obtained by precipitation from cold diethyl ether and subsequent vacuum drying (yield, 93%). ¹H-NMR (400 MHz, CDCl₃): δ 5.30-5.15 (m, 1H, -OC-CH(CH₃)O-, PLGA), 4.95-4.65 (m, 2H, -OC-CH₂O-, PLGA), 1.61 (brs, 3H, -OC-CH(CH₃)O-, PLGA).

Synthesis of PLGA-PEG-NH₂

To a solution of PLGA-NHS (0.50 g, 0.028 mmol) in anhydrous CHCl₃ (2 mL), NH₂-PEG-NH₂ (0.49 g, 0.14 mmol) in anhydrous CHCl₃ (5 mL) and was added DIPEA (0.9 mL, 5.17 mmol), and the solution was magnetically stirred at room temperature for 24 h under nitrogen atmosphere. The PLGA-PEG-NH₂ copolymer was obtained by precipitation with cold diethyl ether, dried under vacuum, and used for NP preparation without further treatment (yield, 89%). ¹H-NMR (400 MHz, CDCl₃): δ 5.30-5.12 (m, 1H, -OC-CH(CH₃)O- PLGA), 4.90-4.62 (m, 2H, -OC-CH₂O- PLGA), 3.65 (brs, 2H, -CH₂CH₂O-, PEG), 1.58 (brs, 3H, -OC-CH(CH₃)O-, PLGA).

Synthesis of PLGA-PEG-12

PLGA-PEG-mal (0.47 g, 0.022 mmol) and peptide KTLLPTPC (**12**, 0.02 g, 0.023 mmol) were dissolved in 15 mL of 1:1 solution of acetonitrile and DMF. The resulting reaction was stirred for 24 h under nitrogen atmosphere. The desired *pseudo*-tri-block-copolymer was obtained by precipitation with cold diethyl ether, then dried under vacuum, and used for NP preparation without further treatment (yield, 88%). ¹H-NMR (400 MHz, CDCl₃): δ 5.28-5.10 (m, 1H, -OC-CH(CH₃)O-, PLGA), 4.88-4.64 (m, 2H, -OC-CH₂O-, PLGA), 3.64 (brs, 2H, -CH₂CH₂O-, PEG), 1.58 (brs, 3H, -OC-CH(CH₃)O-, PLGA).

Synthesis of PLGA-PEG-mal

To a solution of PLGA-NHS (0.51 g, 0.029 mmol) in anhydrous CHCl_3 (3 mL), NH_2 -PEG-maleimide (0.40 g, 0.11 mmol) in anhydrous CHCl_3 (2 mL) and was added DIPEA (0.92 mL, 5.31 mmol), and the solution was magnetically stirred at room temperature for 24 h under nitrogen atmosphere. The PLGA-PEG-mal copolymer was obtained by precipitation with cold diethyl ether, then dried under vacuum, and used for NP preparation without further treatment (yield, 95%). ^1H -NMR (400 MHz, CDCl_3): δ 5.32-5.10 (m, 1H, $-\text{OC}-\text{CH}(\text{CH}_3)\text{O}-$ PLGA), 4.93-4.63 (m, 2H, $-\text{OC}-\text{CH}_2\text{O}-$ PLGA), 3.64 (brs, 2H, $-\text{CH}_2\text{CH}_2\text{O}-$, PEG), 1.58 (brs, 3H, $-\text{OC}-\text{CH}(\text{CH}_3)\text{O}-$, PLGA).

Nanoformulation and characterization of non-targeted and 11- and 12-targeted NPs

Preparation of (1)-loaded PLGA-A and PLGA-11 NPs

Targeted (PLGA-11) and nontargeted (PLGA-A) NPs were prepared using a modified solvent displacement method as previously described.¹⁹ Briefly, polymer (PLGA-A or PLGA-11) (99.5 mg) and **1** (0.5 mg) were co-dissolved in acetonitrile (6.0 mL) and added dropwise into 20 mL of PVA 1% (w/v) solution under rapid magnetic stirring. The resulting suspension was treated as reported,¹⁹ with minimal modifications (ie, centrifugation was conducted at 13000 rpm, and pellets suspended in a minimal volume of water before storage). Batches without **1** were prepared and used as comparison.

Preparation of (1)-loaded PLGA-PEG-NH₂ and PLGA-PEG-12 NPs

The PLGA-PEG-12 conjugate (or the PLGA-PEG-NH₂ copolymer for nontargeted particles) (19.9 mg), PCL (79.6 mg), and **1** (0.5 mg) were co-dissolved in 3 mL of acetonitrile and added dropwise to 3 mL of distilled water under magnetic stirring. Samples were treated as reported above. Batches without **1** were prepared and used for comparison.

Preparation of 6-coumarin-loaded NPs

The preparation of NPs loaded with 6-coumarin was the same as that of NPs without dye, except that 6-coumarin (0.5 mg) was additionally added to acetonitrile containing polymers (total weight 100 mg) before nanoprecipitation.

Characterization of nanoparticles

Morphology, size and zeta potential

The morphology of NPs was characterized by Scanning Electron Microscopy (SEM) (model DSM 962, Carl Zeiss Inc., Jena, Germany). A drop of NPs aqueous suspension was placed on a glass cover slide and dried under vacuum for 12 h. Next, the slides were mounted on aluminum stub and the samples were then analyzed at 20 kV acceleration voltage after gold sputtering, under an argon atmosphere.

Mean diameter and polydispersity index of NPs were measured by using photon correlation spectroscopy (Zetasizer Nano ZS, Malvern Instruments, U.K.) at 25 °C, and a scattering angle of 90° after dilution of samples with Milli-Q water (1.0 mg of NPs / 2.0 mL). Each sample was measured in triplicate.

The zeta potential of the NPs was detected at 25 °C with a Zeta Plus analyzer (Brookhaven, USA). The samples were diluted with distilled water (1.0 mg of NPs / 2.0 mL) and sonicated for several minutes before measurement. All data were obtained with the average of three measurements.

Determination of 1 content and yield of productions

The amount of the encapsulated **1** into NPs was determined by dissolving a weighted amount (10 mg) of dried (**1**)-loaded NPs in CH₂Cl₂ (1 mL), and measured using an HPLC method, according with a procedure previously reported by us,¹⁹ with the following modification: the mobile phase consisting of solvent A/solvent B (60/40 v/v), where solvent A was TFA in water (0.1/99.9 v/v) and solvent B was acetonitrile/water/TFA (95/0.43/0.07 v/v), both prepared daily and degassed by

1
2
3 sonication for 30 min, and filtered before use. Elution was performed at a flow rate of 0.2 mL/min.
4
5 The injection volume was 25 μ L, and the wavelength for UV detection was 255 nm. The total
6
7 analysis time was 20 min, and the retention time of **1** was 8.3 min. The calibration curves were
8
9 found to be linear in the range of 2.5-100 μ g/mL ($y = 777.56x - 303.23$, $R^2 = 0.9999$). The yields of
10
11 production were expressed as the weight percentage of the final product after drying, regarding the
12
13 initial total amount of solid materials used for the preparation.
14

15
16 The amount of 6-coumarin encapsulated was determined using the same procedure already
17
18 described by us,⁴⁸ with UV-vis spectroscopy analysis conducted at 450 nm.
19
20

21 22 23 ***In vitro* kinetics release of **1** from NPs**

24
25 Formulation of PLGA-A, PLGA-**11**, PLGA-PEG-NH₂ and PLGA-PEG-**12** (**1**)-loaded NPs, were
26
27 chosen for the next step of the study. Aliquots of (**1**)-loaded NPs in original suspensions (containing
28
29 about 1.0 μ g of **1**) were dispersed in 2.0 mL of PBS at different pHs (pH 6.5 and pH 7.4) containing
30
31 0.1% w/v Tween-80 (used to improve the solubility of **1** in PBS), and continuously shaken at 37 °C.
32
33 At various time points, the suspension was centrifuged at 13,000 rpm for 2 min, and 1.0 mL
34
35 aliquots of medium were taken from supernatant and replaced with fresh solution. The collected
36
37 samples were extracted with 0.2 mL dichloromethane, evaporated, and reconstituted in 100 μ L
38
39 mobile phase. The concentration of **1** released from the NPs was determined by HPLC assay as
40
41 described above and corrected for the dilution due to the addition of fresh medium.
42
43
44
45
46

47 48 **Cell culture**

49
50 Pancreatic cancer cell line (MIA PaCa-2) was purchased from the American Type Culture
51
52 Collection (Manassas, VA, USA). Cells were maintained in culture under 35 passages and tested
53
54 regularly for *Mycoplasma* contamination using Plasco TestTM (InvivoGen, San Diego, CA, USA).
55
56 MIA PaCa-2 cell line was maintained in appropriate growth media DMEM (Cellgro, Mediatech,
57
58 Manassas, VA, USA) containing 10% heat-inactivated FBS (Gemini- Bioproducts, West
59
60

1
2
3 Sacramento, CA, USA) at 37 °C in a humidified atmosphere of 5% CO₂. For subculture and
4
5 experiments, cells were washed with 1 × Dulbecco's PBS (DPBS, Cellgro), detached using 0.025%
6
7 trypsin-EDTA (Cellgro), collected in growth media and centrifuged. All experiments were
8
9 performed in growth media using sub-confluent cells in the exponential growth phase.
10
11

12 13 14 **Cytotoxicity assay**

15
16 Cytotoxicity was assessed by a 3-(4,5-dimethylthiazol-2-yl)-2,5-diphenyltetrazolium bromide
17
18 (MTT) assay as previously described.¹² Briefly, cells were seeded in 96-well tissue culture treated
19
20 plates and allowed to adhere overnight. Cells were subsequently treated with vehicle or 100 µL of a
21
22 suspension of (1)-loaded NPs in serum-free culture medium to a final concentration of 2.8 µM 1,
23
24 then incubated in medium at 37 °C for required amount of time. After 72 h, MTT (0.3 mg/mL) was
25
26 added to each well. Cells were incubated with MTT for 3 h at 37 °C. After removal of the
27
28 supernatant, DMSO was added and the absorbance was read at 570 nm. All assays were done in
29
30 triplicate. Percent cytotoxicity was calculated by comparing the absorbance from treated wells to
31
32 that of the control wells using following formula: % cytotoxicity = 100 x (1 - [Abs (drug
33
34 treated)/Abs (control)]).
35
36
37
38
39
40

41 **Surface plasmon resonance binding assays**

42
43 Binding experiments were performed using a Biacore T-200 instrument (Biacore, Uppsala, Sweden)
44
45 at 25 °C. 11000 RU of the human Plec-1 partial ORF (4384-4493 a.a.) recombinant protein with
46
47 GST-tag at N-terminal (37.84 kDa, from Abnova Corporation, Taiwan) were directly immobilized
48
49 on the N-ethyl-N-(3-dimethylaminopropyl) carbodiimide (EDC) and N-hydroxysuccinimide (NHS)
50
51 activated flow cell2 of the CM5 chip (GE certified) in water. The flow rate of the 10 mM sodium
52
53 acetate buffer (pH 5.0), used for capturing the protein, was 5 µl/min. The unoccupied sites were
54
55 blocked with 1M ethanolamine.
56
57

58
59 NPs were diluted to 5 mg/ml in standard HBS-N buffer [10 mM HEPES buffer (pH 7.4), 150 mM
60

1
2
3 NaCl, 3 mM EDTA, 0.05% P20 (polyoxyethylenesorbitan), and 1 mg/ml bovine serum albumin
4 (BSA)], sonicated with 5 sec pulses three times and kept on ice until ready. Comparative binding
5 analysis was performed using analyte NPs flowed over the chip at single analyte concentration, with
6 a flow rate of 30 μ l/min. Binding of analyte to the immobilized protein was monitored in real time.
7
8
9
10

11 12 13 14 **Fluorescence Microscopy**

15
16 Cells were seeded in clear bottom black plates and allowed to adhere overnight. Following which
17 cells were treated with indicated samples for 1h at 37 °C. After this, cells were washed with 1x PBS
18 to remove excess nanoparticles and dye. Cells were then imaged using BD Pathway 435 High-
19 Content Bioimager (BD Biosciences) using 20x objective.
20
21
22
23

24
25
26
27 **Statistical analysis.** The data for preparation and characterization of NPs as well as drug release
28 studies were processed and analyzed by Origin software (version 7.0 SR0, OriginLab Corporation,
29 USA). The statistical analysis, evaluated by a Student's *t*-test and *p*-values < 0.05, was considered
30 statistically significant. The data obtained from cytotoxicity assays were processed by One-way
31 analysis of variance (ANOVA) followed by a post-hoc "Newman-Keuls Multiple Comparison Test"
32 to detect differences of means among treatments with significance defined as *p* < 0.05.
33
34
35
36
37
38
39
40
41
42
43
44

45 ASSOCIATED CONTENT

46
47 **Supporting Information.** MS and NMR spectra, elemental analyses, for compounds **1**, **2**, **5**, **6**, **7**,
48 **10**, **11**. NMR spectra for polymers PLGA-**11**, PLGA-PEG-NH₂ and PLGA-PEG-**12**. ¹H-NMR
49 spectrum for peptide **12**. Synthesis and characterization of **12**. Characterization details of 6-
50 coumarin (6C)-loaded NPs. GPC-SEC data (molecular weights, polydispersity and refractive
51 indexes) for PLGA-PEG-NH₂ and PLGA-PEG-**12** polymers.
52
53
54
55
56
57
58
59
60

AUTHOR INFORMATION

Corresponding Authors:

For M.S.: phone, +39 079-228-753; fax: +39 079-229-559, e-mail: mario.sechi@uniss.it

For N.N.: phone, +1 734 647-2732; fax, +1 734 647-8430, e-mail: neamati@umich.edu

Notes

The authors declare no competing financial interest.

ACKNOWLEDGMENTS

The authors gratefully acknowledge the Regione Autonoma della Sardegna for financial support grant CRP 25920, awarded to MS within the frame of “Legge regionale n. 7/2007, promozione della ricerca scientifica e dell’innovazione tecnologica in Sardegna, Annualità 2010”, and the Fondazione Banco di Sardegna for its partial support. The work in NN laboratory was supported by the National Cancer Institute Grant CA188252. The authors thank Dr. Anna Maria Roggio for her help with Mass and HPLC analysis, the Purac Biomaterials (Gorinchem, Netherlands) for providing the PLGA polymer, the Precision AntibodyTM (Columbia, MD, USA), the CASLO Laboratory ApS, c/o Scion Denmark Technical University (Lyngby, Denmark), and the Alfatestlab s.r.l. (MI, Italia) for their helpful technical assistance.

ABBREVIATIONS

NPs, nanoparticles; PLGA, poly-(*D,L*-lactide-*co*-glycolide); PLGA-PEG, poly(*D,L*-lactic-*co*-glycolic acid)-*block*-poly(ethylene glycol); PCL, poly(epsilon-caprolactone); PaCa, Pancreatic Cancer; PDAC, ductal adenocarcinoma; QDs, quinazolinedione-based compounds; ROS, reactive oxygen species; Plec-1, Plectin-1; PTP, KTLTPP peptide; Cys-PTP, KTLTPPC peptide; 2ABA, 2-amino-*N*-(3-aminopropyl)benzamide; TFA, trifluoroacetic acid; Fmoc, fluorenylmethyloxycarbonyl; SPR, surface plasmon resonance; BSA, bovine serum albumin; GPC,

1
2
3 gel permeation chromatography; SEC, size exclusion chromatography; MTT, 3-(4,5-
4 dimethylthiazol-2-yl)-2,5-diphenyltetrazolium bromide; Akt, protein kinase B; Src, proto-oncogene
5 tyrosine-protein kinase; FAK, focal adhesion kinase; STAT3, signal transducer and activator of
6 transcription 3; RES, reticuloendothelial system; PK, pharmacokinetic
7
8
9
10
11
12
13
14
15
16
17
18
19
20
21
22
23
24
25
26
27
28
29
30
31
32
33
34
35
36
37
38
39
40
41
42
43
44
45
46
47
48
49
50
51
52
53
54
55
56
57
58
59
60

References

- [1] Ryan, D. P.; Hong, T. S.; Bardeesy, N. Pancreatic adenocarcinoma. *N. Engl. J. Med.* **2014**, *371*, 1039-1049.
- [2] Siegel, R. L.; Miller, K. D.; Jemal, A. Cancer statistics, **2016**. *CA Cancer J. Clin.* **2016**, *66*, 7-30.
- [3] Malvezzi, M.; Bertuccio, P.; Levi, F.; La Vecchia, C.; Negri, E. European cancer mortality predictions for the year 2014. *Ann. Oncol.* **2014**, *25*, 1650-1656.
- [4] Hidalgo, M. New insights into pancreatic cancer biology. *Ann. Oncol.* **2012**, *23 (Suppl 10)*, x135-x138.
- [5] Hidalgo, M. Pancreatic cancer. *N. Engl. J. Med.* **2010**, *362*, 1605-1617.
- [6] Conroy, T.; Desseigne, F.; Ychou, M.; Bouche, O.; Guimbaud, R.; Becouarn, Y.; Adenis, A.; Raoul, J. L.; Gourgou-Bourgade, S.; de la Fouchardiere, C.; Bennouna, J.; Bachet, J. B.; Khemissa-Akouz, F.; Pere-Verge, D.; Delbaldo, C.; Assenat, E.; Chauffert, B.; Michel, P.; Montoto-Grillot, C.; Ducreux, M.; Groupe Tumeurs Digestives of, U.; Intergroup, P. FOLFIRINOX versus gemcitabine for metastatic pancreatic cancer. *N. Engl. J. Med.* **2011**, *364*, 1817-1825.
- [7] Di Marco, M.; Di Cicilia, R.; Macchini, M.; Nobili, E.; Vecchiarelli, S.; Brandi, G.; Biasco, G. Metastatic pancreatic cancer: is gemcitabine still the best standard treatment? (Review). *Oncol. Rep.* **2010**, *23*, 1183-1192.
- [8] Von Hoff, D. D.; Ervin, T.; Arena, F. P.; Chiorean, E. G.; Infante, J.; Moore, M.; Seay, T.; Tjulandin, S. A.; Ma, W. W.; Saleh, M. N.; Harris, M.; Reni, M.; Dowden, S.; Laheru, D.; Bahary, N.; Ramanathan, R. K.; Tabernero, J.; Hidalgo, M.; Goldstein, D.; Van Cutsem, E.; Wei, X.; Iglesias, J.; Renschler, M. F. Increased survival in pancreatic cancer with nab-paclitaxel plus gemcitabine. *N. Engl. J. Med.* **2013**, *369*, 1691-1703.
- [9] Srinivasarao, M.; Galliford, C. V.; Low, P. S. Principles in the design of ligand-targeted cancer therapeutics and imaging agents. *Nat. Rev. Drug. Discov.* **2015**, *14*, 203-219.
- [10] Byrne, J. D.; Betancourt, T.; Brannon-Peppas, L. Active targeting schemes for nanoparticle systems in cancer therapeutics. *Adv. Drug. Deliv. Rev.* **2008**, *60*, 1615-1626.
- [11] Lammers, T.; Kiessling, F.; Hennink, W. E.; Storm, G. Drug targeting to tumors: principles, pitfalls and (pre-) clinical progress. *J. Control. Release* **2012**, *161*, 175-187. □
- [12] Pathania, D.; Sechi, M.; Palomba, M.; Sanna, V.; Berrettini, F.; Sias, A.; Taheri, L.; Neamati, N. Design and discovery of novel quinazolinone-based redox modulators as therapies for pancreatic cancer. *Biochim. Biophys. Acta* **2014**, *1840*, 332-343.
- [13] Pathania, D.; Kuang, Y.; Sechi, M.; Neamati, N. Mechanisms underlying the cytotoxicity of a novel quinazolinone-based redox modulator, QD232, in pancreatic cancer cells. *Br. J. Pharmacol.* **2015**, *172*, 50-63.

- 1
2
3 [14] Hanahan, D.; Weinberg, R. A. Hallmarks of cancer: the next generation. *Cell* **2011**, *144*,
4 646-674.
5
6 [15] Pathania, D.; Millard, M.; Neamati, N. Opportunities in discovery and delivery of anticancer
7 drugs targeting mitochondria and cancer cell metabolism. *Adv. Drug Deliv. Rev.* **2009**, *61*, 1250-
8 1275.
9
10 [16] Storz, P. Reactive oxygen species in tumor progression. *Front. Biosci.* **2005**, *10*, 1881-1896.
11
12 [17] Shackelford, R. E.; Kaufmann, W. K.; Paules, R. S. Oxidative stress and cell cycle
13 checkpoint function. *Free Radic. Biol. Med.* **2000**, *28*, 1387-1404.
14
15 [18] Trachootham, D.; Alexandre, J.; Huang, P. Targeting cancer cells by ROS-mediated
16 mechanisms: a radical therapeutic approach? *Nat. Rev. Drug Discov.* **2009**, *8*, 579-591.
17
18 [19] Sanna, V.; Pintus, G. P.; Roggio, A. M.; Punzoni, S.; Posadino, A. M.; Arca, A.; Marceddu,
19 S.; Bandiera, P.; Uzzau, S.; Sechi, M. Targeted biocompatible nanoparticles for the delivery of (-)-
20 epigallocatechin 3-gallate to prostate cancer cells. *J. Med. Chem.* **2011**, *54*, 1321-1332.
21
22 [20] Davis, M. E.; Chen, Z. G.; Shin, D. M. Nanoparticle therapeutics: an emerging treatment
23 modality for cancer. *Nat. Rev. Drug Discov.* **2008**, *7*, 771-782.
24
25 [21] Peer, D.; Karp, J. M.; Hong, S.; Farokhzad, O. C.; Margalit, R.; Langer, R. Nanocarriers as
26 an emerging platform for cancer therapy. *Nat. Nanotechnol.* **2007**, *2*, 751-760.
27
28 [22] Farokhzad, O. C.; Langer, R. Impact of nanotechnology on drug delivery. *ACS Nano* **2009**,
29 *3*, 16-20.
30
31 [23] Nicolas, J.; Mura, S.; Brambilla, D.; Mackiewicz, N.; Couvreur, P. Design, functionalization
32 strategies and biomedical applications of targeted biodegradable/biocompatible polymer-based
33 nanocarriers for drug delivery. *Chem. Soc. Rev.* **2013**, *42*, 1147-1235.
34
35 [24] Shi, J.; Xiao, Z.; Kamaly, N.; Farokhzad, O. C. Self-assembled targeted nanoparticles:
36 evolution of technologies and bench to bedside translation. *Acc. Chem. Res.* **2011**, *44*, 1123-1134.
37
38 [25] Sanna, V.; Pala, N.; Sechi, M. Targeted therapy using nanotechnology: focus on cancer. *Int.*
39 *J. Nanomedicine* **2014**, *9*, 467-483.
40
41 [26] Gu, F.; Langer, R.; Farokhzad, O. C. Formulation/preparation of functionalized
42 nanoparticles for in vivo targeted drug delivery. *Methods Mol. Biol.* **2009**, *544*, 589-598.
43
44 [27] Alexis, F.; Pridgen, E. M.; Langer, R.; Farokhzad, O. C. Nanoparticle technologies for
45 cancer therapy. *Handb. Exp. Pharmacol.* **2010**, *197*, 55-86.
46
47 [28] Kamaly, N.; Xiao, Z.; Valencia, P. M.; Radovic-Moreno, A. F.; Farokhzad, O. C. Targeted
48 polymeric therapeutic nanoparticles: design, development and clinical translation. *Chem. Soc. Rev.*
49 **2012**, *41*, 2971-3010.
50
51
52
53
54
55
56
57
58
59
60

- 1
2
3 [29] Siu, D. Cancer therapy using tumor-associated antigens to reduce side effects. *Clin. Exp.*
4 *Med.* **2009**, *9*, 181-198.
- 5
6 [30] Steinbock, F. A.; Wiche, G. Plectin: a cytolinker by design. *Biol. Chem.* **1999**, *380*, 151-158.
- 7
8 [31] Bausch, D.; Thomas, S.; Mino-Kenudson, M.; Fernandez-del, C. C.; Bauer, T. W.; Williams,
9 M.; Warshaw, A. L.; Thayer, S. P.; Kelly, K. A. Plectin-1 as a novel biomarker for pancreatic
10 cancer. *Clin. Cancer Res.* **2011**, *17*, 302-309.
- 11
12 [32] Kelly, K. A.; Bardeesy, N.; Anbazhagan, R.; Gurumurthy, S.; Berger, J.; Alencar, H.;
13 Depinho, R. A.; Mahmood, U.; Weissleder, R. Targeted nanoparticles for imaging incipient
14 pancreatic ductal adenocarcinoma. *PLoS Med.* **2008**, *5*, e85.
- 15
16 [33] Weissleder, R.; Kelly, K.; Sun, E. Y.; Shtatland, T.; Josephson, L. Cell-specific targeting of
17 nanoparticles by multivalent attachment of small molecules. *Nat. Biotechnol.* **2005**, *23*, 1418-1423.
- 18
19 [34] Langer, R.; Folkman, J. Polymers for the sustained release of proteins and other
20 macromolecules. *Nature* **1976**, *263*, 797-800. □
- 21
22 [35] Gref, R.; Minamitake, Y.; Peracchia, M. T.; Trubetskoy, V.; Torchilin, V.; Langer, R.
23 Biodegradable long-circulating polymeric nanospheres. *Science* **1994**, *263*, 1600-1603.
- 24
25 [36] Farokhzad, O. C.; Cheng, J.; Teply, B. A.; Sherifi, I.; Jon, S.; Kantoff, P. W.; Richie, J. P.;
26 Langer, R. Targeted nanoparticle-aptamer bioconjugates for cancer chemotherapy in vivo. *Proc.*
27 *Natl. Acad. Sci. U.S. A.* **2006**, *103*, 6315-6320.
- 28
29 [37] Gu, F.; Zhang, L.; Teply, B. A.; Mann, N.; Wang, A.; Radovic- Moreno, A. F.; Langer, R.;
30 Farokhzad, O. C. Precise engineering of targeted nanoparticles by using self-assembled
31 biointegrated block copolymers. *Proc. Natl. Acad. Sci. U.S.A.* **2008**, *105*, 2586-2591.
- 32
33 [38] Gu, F.; Langer, R.; Farokhzad, O. C. Formulation/preparation of functionalized
34 nanoparticles for in vivo targeted drug delivery. *Methods Mol Biol.* **2009**, *544*, 589-598.
- 35
36 [39] Otsuka, H.; Nagasaki, Y.; Kataoka, K. PEGylated nanoparticles for biological and
37 pharmaceutical applications. *Adv. Drug. Deliv. Rev.* **2003**, *55*, 403-419.
- 38
39 [40] Avgoustakis, K. PEGylated poly(lactide) and poly(lactide-coglycolide) nanoparticles:
40 Preparation, properties and possible applications in drug delivery. *Curr. Drug. Deliv.* **2004**, *1*, 321-
41 333.
- 42
43 [41] Betancourt, T.; Byrne, J. D.; Sunaryo, N.; Crowder, S. W.; Kadapakkam, M.; Patel, S.;
44 Casciato, S.; Brannon-Peppas, L. PEGylation strategies for active targeting of PLA/PLGA
45 nanoparticles. *J. Biomed. Mater. Res. A.* **2009**, *91*, 263-276.
- 46
47 [42] Cheng, J.; Teply, B. A.; Sherifi, I.; Sung, J.; Luther, G.; Gu, F. X.; Levy-Nissenbaum, E.;
48 Radovic-Moreno, A. F.; Langer, R.; Farokhzad, O. C. Formulation of functionalized PLGA-PEG
49 nanoparticles for in vivo targeted drug delivery. *Biomaterials* **2007**, *28*, 869-876.
- 50
51
52
53
54
55
56
57
58
59
60

- 1
2
3 [43] Alexis, F.; Pridgen, E.; Molnar, L. K.; Farokhzad, O. C. Factors affecting the clearance and
4 biodistribution of polymeric nanoparticles. *Mol. Pharm.* **2008**, *5*, 505-515.
5
6 [44] Maeda, H.; Wu, J.; Sawa, T.; Matsumura, Y.; Hori, K. Tumor vascular permeability and the
7 EPR effect in macromolecular therapeutics: a review. *J. Control. Release* **2000**, *65*, 271-284.
8
9 [45] Jain, R. K.; Stylianopoulos, T. Delivering nanomedicine to solid tumors. *Nat. Rev. Clin.*
10 *Oncol.* **2010**, *7*, 653-664.
11
12 [46] Danquah, M. K.; Zhang, X. A.; Mahato, R. I. Extravasation of polymeric nanomedicines
13 across tumor vasculature. *Adv. Drug Deliv. Rev.* **2011**, *63*, 623-639. □
14
15 [47] Knop, K.; Hoogenboom, R.; Fischer, D.; Schubert US. Poly(ethylene glycol) in drug
16 delivery: pros and cons as well as potential alternatives. *Angew. Chem. Int. Ed. Engl.* **2006**, *49*,
17 6288–6308.
18
19 [48] Jokerst, J. V.; Lobovkina, T.; Zare, R. N.; Gambhi, S. S. Nanoparticle PEGylation for
20 imaging and therapy. *Nanomedicine (Lond.)* **2011**, *6*, 715–728.
21
22 [49] Dash, T. K.; Konkimalla, V. B. Polymeric modification and its implication in drug delivery:
23 poly- ϵ -caprolactone (PCL) as a model polymer. *Mol. Pharm.* **2012**, *9*, 2365-2379.
24
25 [50] Sanna, V.; Siddiqui, I. A.; Sechi, M.; Mukhtar, H. Resveratrol-loaded nanoparticles based on
26 poly(ϵ -caprolactone) and poly(D,L-lactic-co-glycolic acid)-poly(ethylene glycol) blend for
27 prostate cancer treatment. *Mol. Pharm.* **2013**, *10*, 3871-3881.
28
29 [51] Sanna, V.; Roggio, A. M.; Posadino, A. M.; Cossu, A.; Marceddu, S.; Mariani, A.; Alzari,
30 V.; Uzzau, S.; Pintus, G.; Sechi, M. Novel docetaxel-loaded nanoparticles based on poly(lactide-co-
31 caprolactone) and poly(lactide-co-glycolide-co-caprolactone) for prostate cancer treatment:
32 formulation, characterization and cytotoxicity studies. *Nanoscale Res. Lett.* **2011**, *6*(1), 260.
33
34 [52] Patching, S. G. Surface plasmon resonance spectroscopy for characterisation of membrane
35 protein-ligand interactions and its potential for drug discovery. *Biochim. Biophys. Acta* **2014**, *1838*,
36 43-55.
37
38
39
40
41
42
43
44
45
46
47
48
49
50
51
52
53
54
55
56
57
58
59
60

Figures, Schemes and Tables Legends

Figure 1. Schematic representation of the designed targeted PLGA-**11**- and PLGA-PEG-**12**-**(1)**-loaded NPs. Materials: chemical structure of QD242 (**1**), the low molecular weight organic molecule targeting ligand 2ABA (**11**), the cysteine-containing Plec-1 targeting peptide Cys-PTP (**12**), PLGA and PLGA-PEG polymers.

Figure 2. Characterization of PLGA-**11** polymer. UV spectra comparison of PLGA-NHS (black line), **11** (red line), and PLGA-**11** (blue line).

Figure 3. Characterization of PLGA-PEG-**12** polymer. UV spectra comparison of PLGA-PEG-mal (green line), **12** (red line), and PLGA-PEG-**12** (blue line).

Figure 4. SEM images of PLGA-A- (a), PLGA-**11**- (b), PLGA-PEG-NH₂/PCL- (c), and PLGA-PEG-**12**/PCL- (d) (**1**)-loaded NPs and corresponding particle size distribution. The scale bar is 200 nm.

Figure 5. *In vitro* release profiles of **1** from nontargeted (PLGA-A and PLGA-PEG-NH₂) and targeted (PLGA-**11** and PLGA-PEG-**12**) NPs, detected at pH 6.5 (a) and 7.4 (b).

Figure 6. *In vitro* cytotoxicity of nontargeted (PLGA-A, PLGA-PEG-NH₂), and targeted (PLGA-**11** and PLGA-PEG-**12**) NPs. MIA PaCa-2 cell treated with (**1**)-loaded NPs (**1**, 2.8 μM) for 72 h. (*) significantly differ from each other.

Figure 7. Surface plasmon resonance (SPR)-based comparative binding analysis of ligand-functionalized NPs. Sensorgrams showing binding of targeted PLGA-PEG-**12** and

1
2
3 nontargeted PLGA-PEG-NH₂ NPs to Plec-1 protein. The experiment was performed
4
5 using a Biacore T-200 system. Plec-1 was directly immobilized in the sensor chip by
6
7 amine coupling (at 11000 RU), and NPs was flowed over the protein-coated chip at 5
8
9 mg/mL in assay buffer, with single cycle kinetics. Lines represent the best fitting of
10
11 the association-dissociation processes for targeted NPs (green line) and nontargeted
12
13 NPs (blue line). Standard HBS-N buffer with 1 mg/mL BSA (pink line) was used as
14
15 control. Data for affinity evaluation were obtained and expressed as difference in
16
17 response units (RU). Data shown are representative of three independent
18
19 experiments.
20
21
22
23
24

25 **Figure 8.** Uptake assays for NPs. Panels show representative live cell fluorescence microscopy
26
27 images of MIA PaCa-2 cells after exposure to nontargeted (PLGA-A, PLGA-PEG-
28
29 NH₂), and targeted (PLGA-**11** and PLGA-PEG-**12**) dye-loaded NPs. Left panels:
30
31 cells incubated with dye-loaded NPs for 1 h. Middle panels: red fluorescence of the
32
33 nuclei stained with DRAQ5 dye. Right panels: cellular uptake visualized by
34
35 overlaying images (20x magnification).
36
37
38
39
40
41
42

43 **Scheme 1.** Synthetic route for the preparation of **1**.
44
45
46

47 **Scheme 2.** Synthetic route for the preparation of ligand **11**.
48
49
50

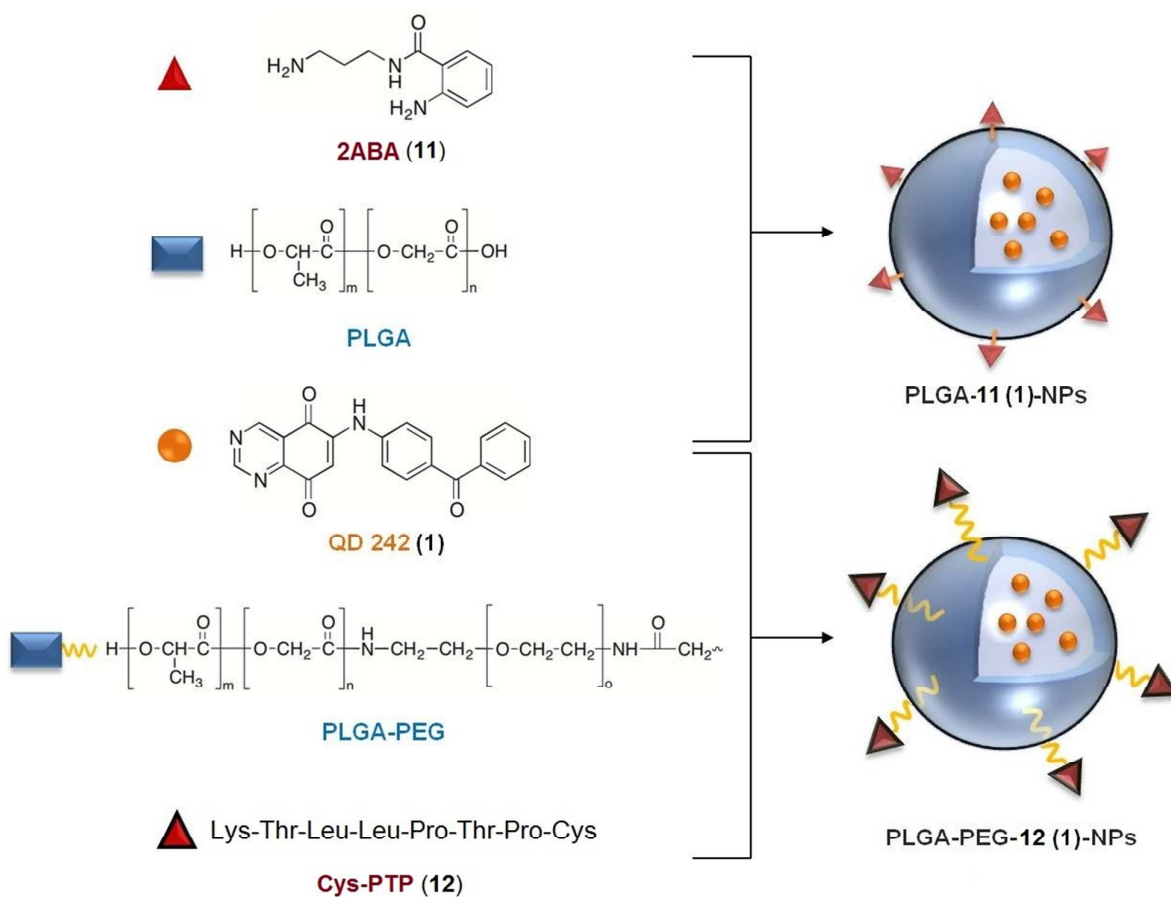
51 **Scheme 3.** Synthesis of copolymer PLGA-**11** (Stage 1) and nanoformulation (Stage 2).
52
53
54
55

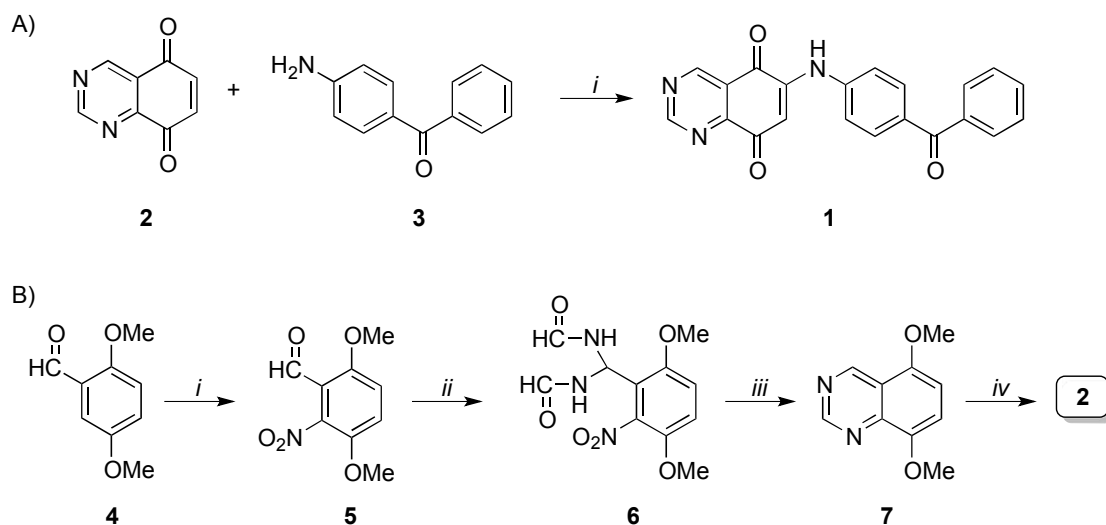
56 **Scheme 4.** Synthesis of copolymer PLGA-PEG-NH₂.
57
58
59
60

1
2
3 **Scheme 5.** Synthesis of copolymer PLGA-PEG-**12** (Stage 1) and nanoformulation (Stage 2).
4
5
6
7
8

9 **Table 1.** Average diameter, polydispersity index, zeta potential, encapsulation efficiency and
10
11 yield of production of (**1**)-loaded NPs.
12
13
14
15
16
17
18
19
20
21
22
23
24
25
26
27
28
29
30
31
32
33
34
35
36
37
38
39
40
41
42
43
44
45
46
47
48
49
50
51
52
53
54
55
56
57
58
59
60

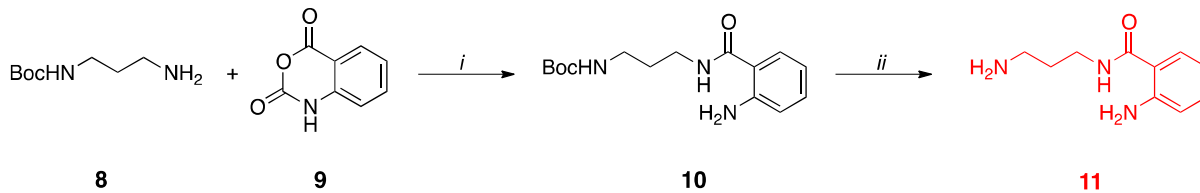
Figure 1. Schematic representation of the designed targeted PLGA-11- and PLGA-PEG-12- (1)-loaded NPs. Materials: chemical structure of QD242 (1), the low molecular weight organic molecule targeting ligand 2ABA (11), the cysteine-containing Plec-1 targeting peptide Cys-PTP (12), PLGA and PLGA-PEG polymers.



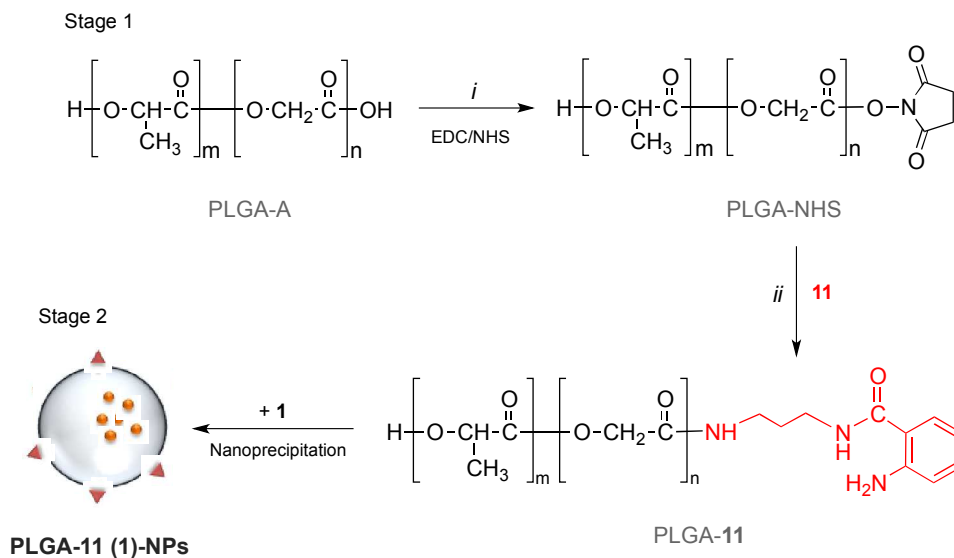
Scheme 1. Synthetic route for the preparation of **1**.^a

^a**Reagents and conditions:** **A**) (i) $\text{CeCl}_3 \cdot 7\text{H}_2\text{O}$, abs EtOH, O_2 , room temp, 3 h. **B**) (i) conc. HNO_3 , $(\text{CH}_3\text{CO})_2\text{O}$, 0°C , 1.5 h; (ii) H_2NCHO , $\text{HCl}_{(\text{g})}$, from 40 to 80°C , 1 h; (iii) glacial CH_3COOH , Zn, 0°C for 2 h, room temp for 4 h; (iv) $(\text{NH}_4)_2\text{Ce}(\text{NO}_3)_6$, $\text{CH}_3\text{CN}/\text{H}_2\text{O}$, 0°C , 20 min.

1
2
3 **Scheme 2.** Synthetic route for the preparation of ligand **11**.^a
4
5
6
7
8
9

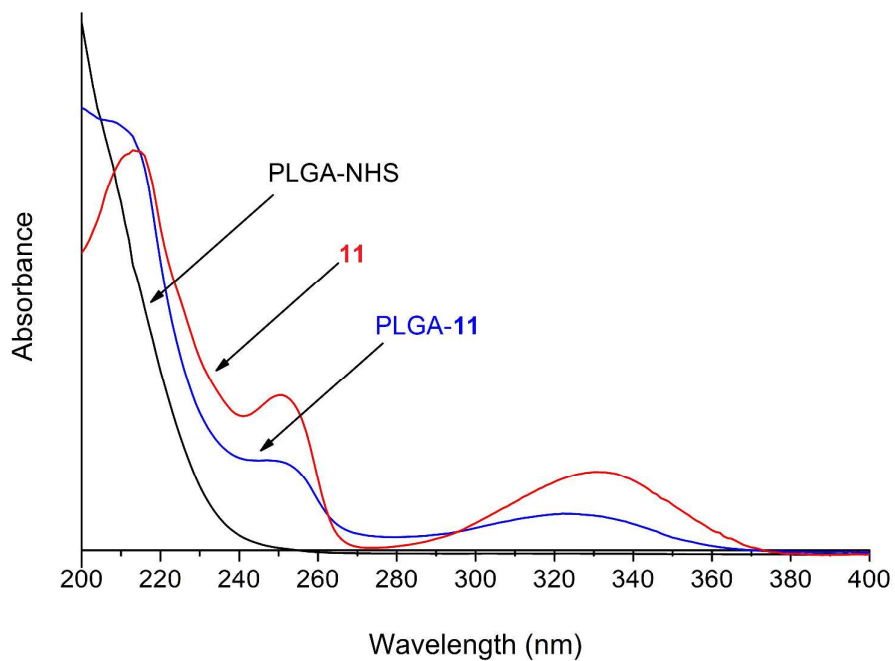


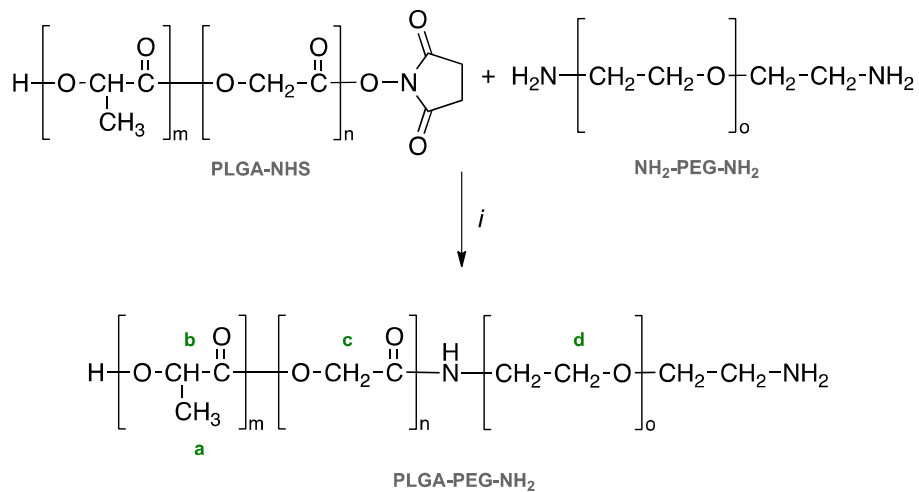
^a**Reagents and conditions:** (i) K_2CO_3 , THF, N_2 , 70 °C for 20 h; (ii) TFA:CH₂Cl₂ (1:1), 0 °C for 3 h.

Scheme 3. Synthesis of copolymer PLGA-11 (Stage 1) and nanoformulation (Stage 2).^a

^a**Reagents and conditions:** (i) NHS, CH₂Cl₂, EDC, N₂, room temp for 12 h; (ii) **11**, DIPEA, DMF, N₂, room temp for 24 h.

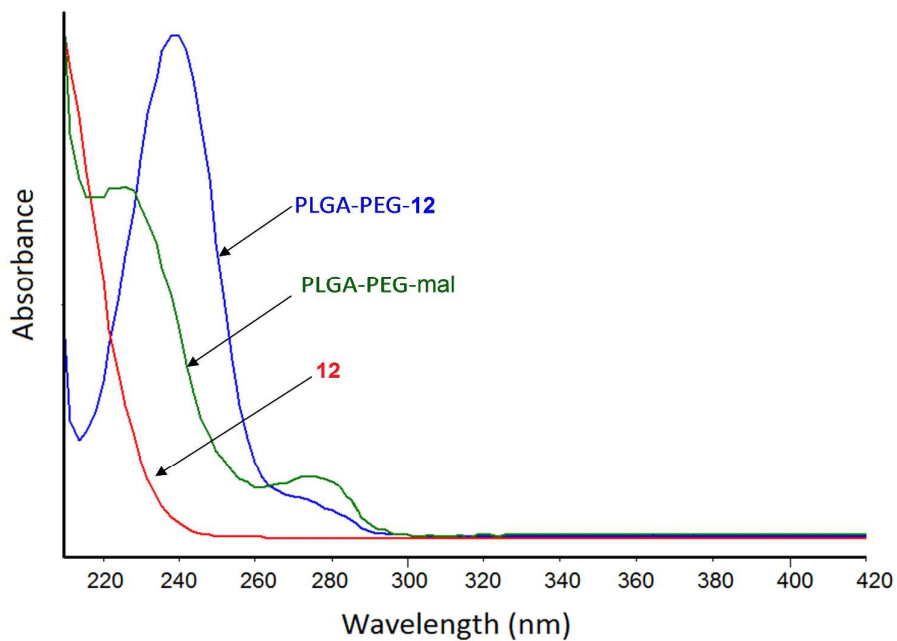
Figure 2. Characterization of PLGA-11 polymer. UV spectra comparison of PLGA-NHS (black line), 11 (red line), and PLGA-11 (blue line).



Scheme 4. Synthesis of copolymer PLGA-PEG-NH₂.^a

^aReagents and conditions: (i) CHCl₃, DIPEA, N₂, room temp for 24 h.

Figure 3. Characterization of PLGA-PEG-12 polymer. UV spectra comparison of PLGA-PEG-mal (green line), 12 (red line), and PLGA-PEG-12 (blue line).



1
2
3 **Figure 4.** SEM images of PLGA-A- (a), PLGA-11- (b), PLGA-PEG-NH₂/PCL- (c), and PLGA-
4
5 PEG-12/PCL- (d) (1)-loaded NPs and corresponding particle size distribution. The scale bar is 200
6
7 nm.
8
9
10
11
12
13
14
15
16
17
18
19
20
21
22
23
24
25
26
27
28
29
30
31
32
33
34
35
36
37
38
39
40
41
42
43
44
45
46
47
48
49
50
51
52
53
54
55
56
57
58
59
60

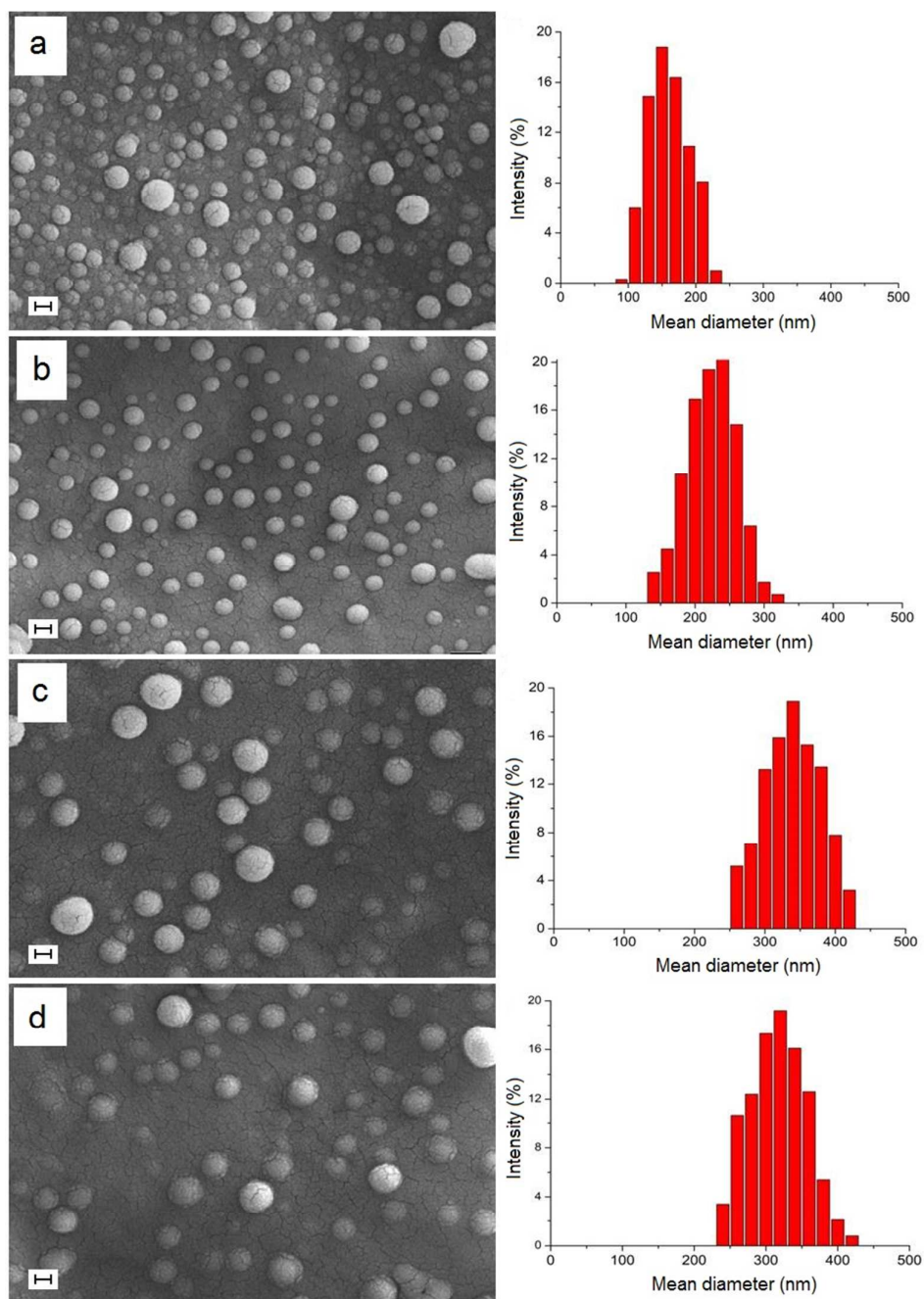


Table 1. Average diameter, polydispersity index, zeta potential, encapsulation efficiency and yield of production of (1)-loaded NPs.

Formulation	Average diameter (nm)	Polydispersity index	Zeta Potential (mV)	Encapsulation efficiency (%)	Yield of production (%)
PLGA-A	155.8±11.6 [°]	0.09±0.01	-20.3±1.2	14.33±1.35 [°]	55.22±6.82 [°]
PLGA-11	220.1±16.6 [°]	0.11±0.02	13.6±1.3	16.49±2.53 [°]	50.60±1.60 [°]
^a PLGA-PEG-NH ₂	353.5±27.0	0.15±0.01	14.1±2.1	20.12±2.47*	69.21±2.35*
^a PLGA-PEG-12	328.0±30.7	0.12±0.03	10.2±1.9	24.52±0.36*	64.03±2.81*

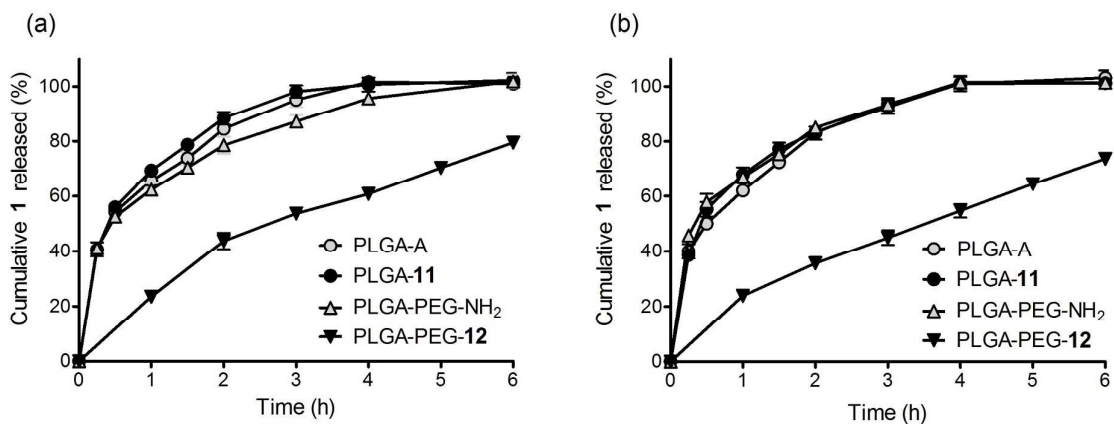
^aFormulation been performed with the addition of PCL polymer (see on the experimental section).

Values presented are the mean ± SD of three preparations.

([°]) Significant differences from PLGA-PEG batches (p < 0.05).

(*) Significant differences from each other (p < 0.05).

Figure 5. *In vitro* release profiles of **1** from nontargeted (PLGA-A and PLGA-PEG-NH₂) and targeted (PLGA-11 and PLGA-PEG-12) NPs, detected at pH 6.5 (a) and 7.4 (b).



1
2
3 **Figure 6.** *In vitro* cytotoxicity of nontargeted (PLGA-A, PLGA-PEG-NH₂), and targeted (PLGA-11
4 and PLGA-PEG-12) NPs. MIA PaCa-2 cell treated with (1)-loaded NPs (1, 2.8 μM) for 72 h. (*)
5 significantly differ from each other.
6
7
8
9

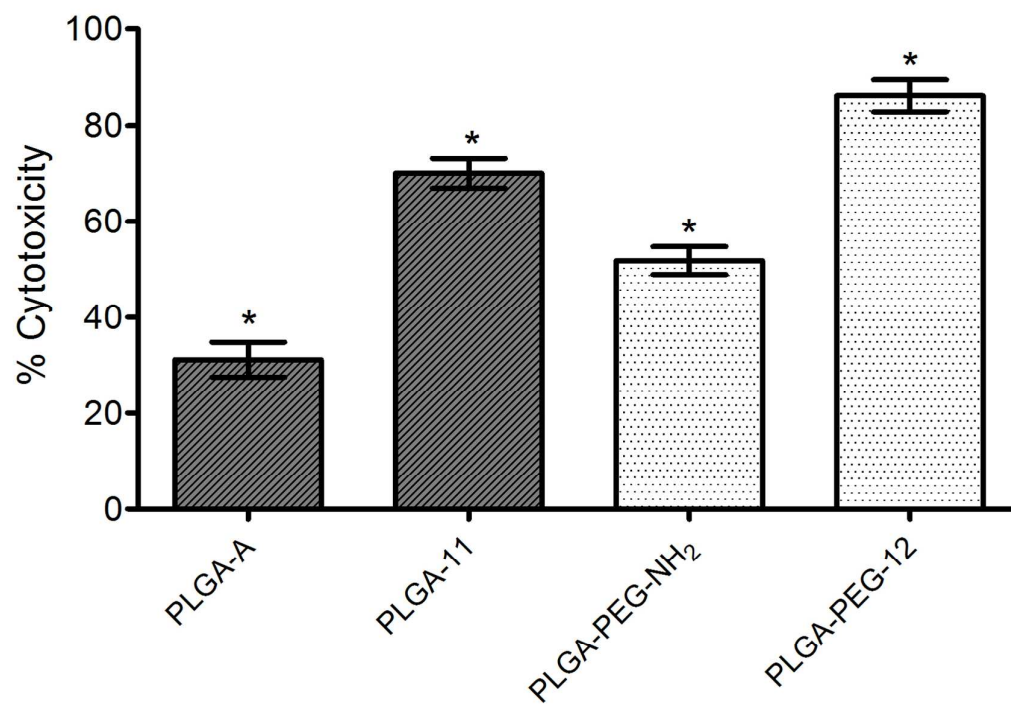


Figure 7. Surface plasmon resonance (SPR)-based comparative binding analysis of ligand-functionalized NPs. Sensorgrams showing binding of targeted PLGA-PEG-12 and nontargeted PLGA-PEG-NH₂ NPs to Plec-1 protein. The experiment was performed using a Biacore T-200 system. Plec-1 was directly immobilized in the sensor chip by amine coupling (at 11000 RU), and NPs was flowed over the protein-coated chip at 5 mg/mL in assay buffer, with single cycle kinetics. Lines represent the best fitting of the association-dissociation processes for targeted NPs (green line) and nontargeted NPs (blue line). Standard HBS-N buffer with 1 mg/mL BSA (pink line) was used as control. Data for affinity evaluation were obtained and expressed as difference in response units (RU). Data shown are representative of three independent experiments.

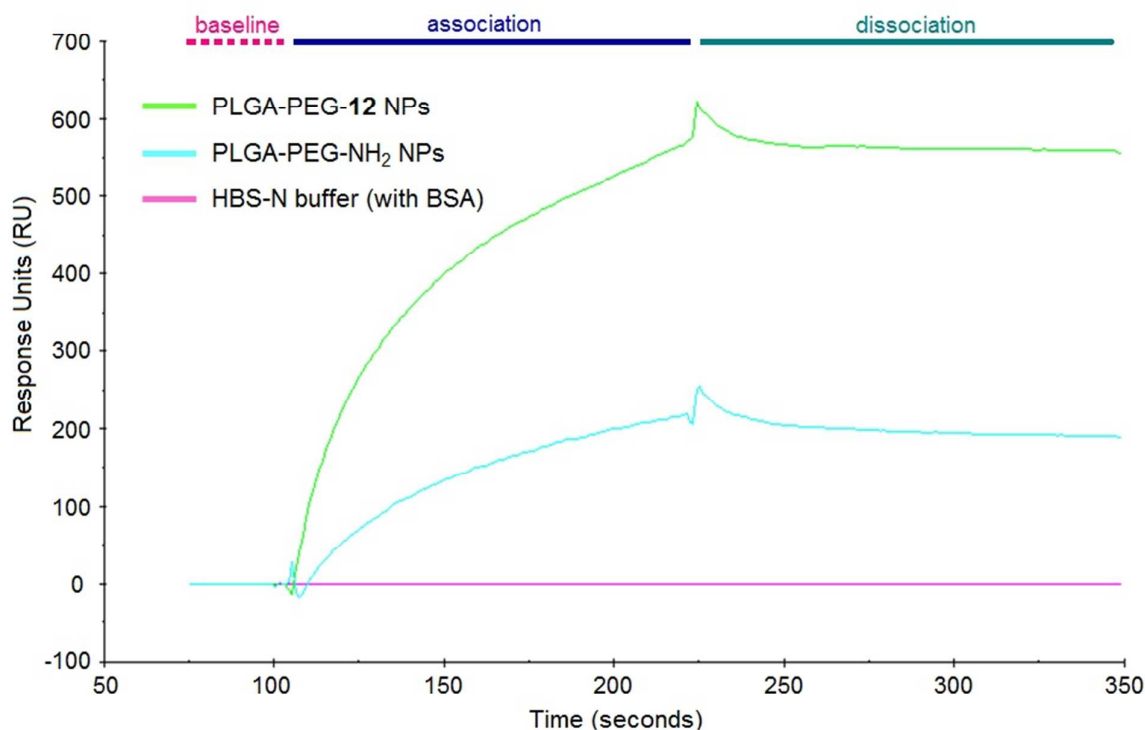


Figure 8. Uptake assays for NPs. Panels show representative live cell fluorescence microscopy images of MIA PaCa-2 cells after exposure to nontargeted (PLGA-A, PLGA-PEG-NH₂), and targeted (PLGA-11 and PLGA-PEG-12) dye-loaded NPs. Left panels: cells incubated with dye-loaded NPs for 1 h. Middle panels: red fluorescence of the nuclei stained with DRAQ5 dye. Right panels: cellular uptake visualized by overlaying images (20x magnification).

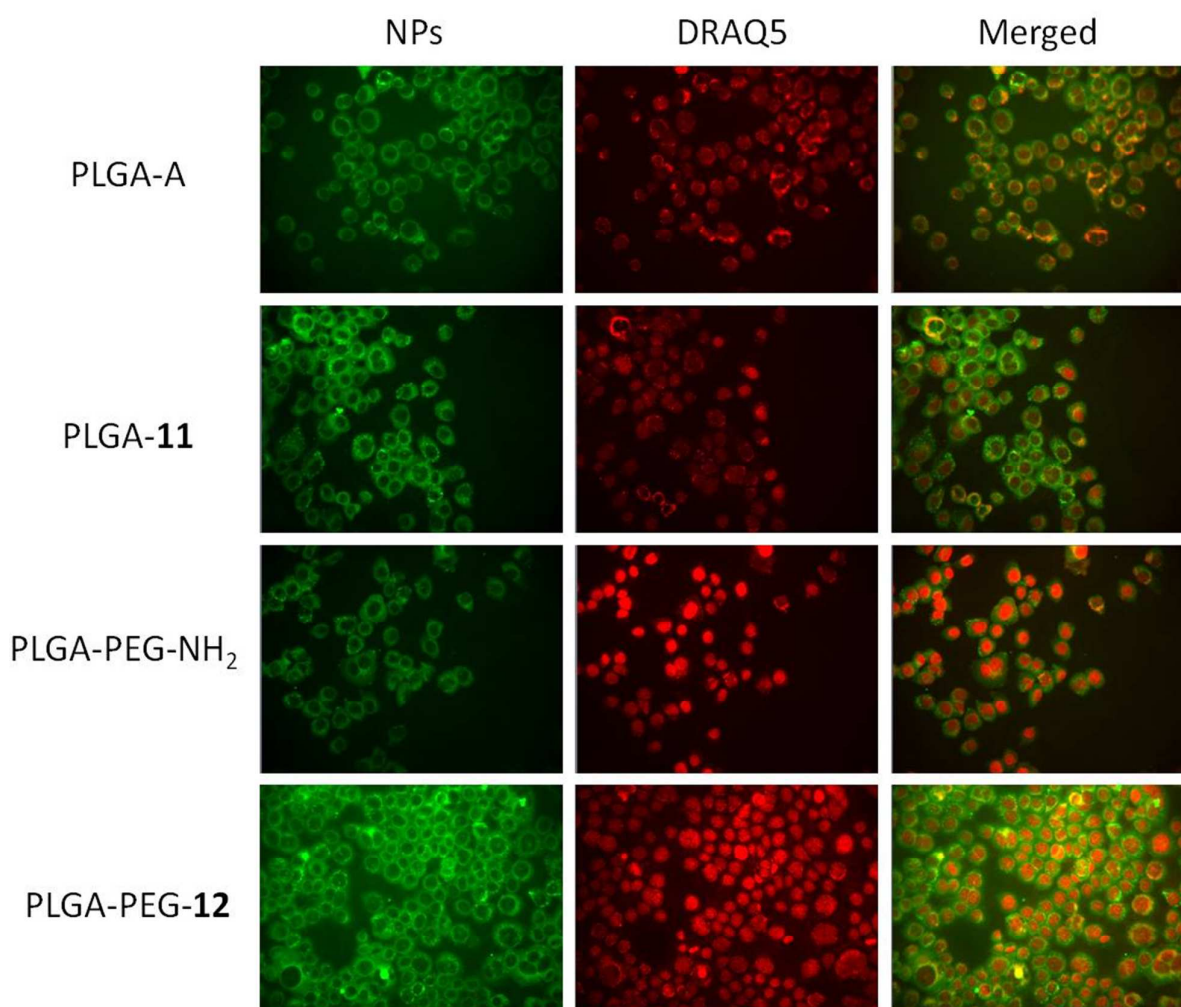


Table of Contents Graphic (TCG)

